OLCI Level 2

Algorithm Theoretical Basis Document

Ocean Colour Turbid Water

Document Ref: S3-L2-SD-03-C11-GKSS-ATBD

Deliverable Ref: SD-03-C11

Version: 2.0

Roland Doerffer

GKSS Research Center

Institute for Coastal Research

Max-Planck-Str. 1

D-21502 Geesthacht

roland.doerffer@gkss.de

Title:

S3-L2-SD-03-C11-GKSS-ATBD_OceanColourTurbidWater_v2.1-100715

Document Ref: S3-L2-SD-03-C11-GKSS-ATBD

	Name	Function	Company	Signature	Date
Prepared	Doerffer		GKSS		20090404
Approved					
Released					

Change Record

Issue	Date	Description	Change Chapters
1.0	04/04/2009	version 1	
1.01	25/09/2009	extended by chapters 5,6, clarification alternative atmospheric correction branch in chapters 3.1.7 and 6.2	chapters 3.1.7 and 6.2
2.0	08/04/2010	extension by using temperature and salinity effects as input to compute pure water optical properties and to train and use the neural network accordingly references	chapter 3.1.2.1, 3.1.5.1, 6.1, 6.2, 7 Fig. 18-20
2.1	15/07/2010	- extension of ch. 3.1.7.5 to justify the alternative atmospheric correction	3.1.7.5

Issue	Date	Description	Change Chapters
		- new chapter 7 (output products)	7
		-new chapter 8 (validation)	8
		- a figure was included in ch. (Fig. 19)	5

Distribution List

Organisation	To	No. copies
ARGANS	S. Lavender	
ESA	P. Goryl	

Table of Content

	SENTINEL-3 L2 PRODUCTS AND ALGORITHM DEFINITION OLCI L2 ATBD Ocean Colour Turbid Water	Document Ref: S3-L2-SD-03-C11-GKSS-ATBD Issue: 2.1 Date: 20100715 Page 5 of 50

GKSS
FORSCHUNGSZENTRUM
in der HELMHOLTZ-GEMEINSCHAFT

List of Figures

1   INTRODUCTION

1.1   Acronyms and Abbreviations

AOP: Apparent optical property

CDOM: coloured dissolved organic matter

ESA; European Space Agency

IOP: inherent optical property

MERIS: Medium Resolution Imaging Spectrometer (on board ENVISAT)

OLCI: Ocean Land Colour Imager

1.2   Purpose and Scope

This ATBD describes the algorithm for the determination of inherent optical properties (IOPs) and the concentration of water constituents in case 2 waters from water leaving radiance reflectance spectra to be used for the Ocean and Land Colour Imager (OLCI) of the Earth Observation Mission SENTINEL 3 of the European Space Agency (ESA).

1.3   Algorithm Identification

OLCI Case 2 Turbid Water Algorithm

2   ALGORITHM OVERVIEW

2.1   Objectives

Objective of this algorithm is to determine optical properties and the concentrations of consti-tuents of case 2 waters from directional water leaving radiance reflectance spectra of OLCI. Case 2 water is defined as a natural water body, which contains more than 1 component of water constituents, which determine the variability of the spectrum of the water leaving radiance.

This type of water is mainly present in coastal seas, estuaries, lagoons and inland waters. Here complex mixtures of different water constituents, including phytoplankton, mineralic and organic suspended matter, dissolved organic matter etc, occur in high concentrations. These constituents have different spectral inherent optical properties, i.e. spectral absorption and

scattering coefficients and partly show inelastic scattering, which determine the light field in the water and the water leaving radiance.

Since there is a high interest by science, environmental monitoring agencies and fishery managers to use remote sensing data, the Sentinel - 3 mission plans to provide the required information about case 2 water properties.

A major problem in case 2 water remote sensing is that the composition of water constituents and their optical properties vary from area to area and partly also by season. Thus, it was necessary to construct a generic algorithm, which is valid in different water types and which allows a regional adaptation for the user.

By following the heritage of MERIS we have chosen an artificial neural network (NN) as a multiple non-linear regression technique. The NN converts the directional water leaving radiance reflectance into a number of inherent optical properties, which - in a further step - can be converted into concentrations of water constituents by simple regressions.

The coefficients of the NN are determined by the training process. For the training and testing a large set of simulated directional water leaving radiance reflectances (RLw) are used. For their simulation a complex radiative transfer model is used, which, again, includes a bio-optical model. The bio-optical model describes the inherent optical properties, i.e. spectral scattering and absorption coefficients as well as the scattering phase functions of pure water and of a number of components, which represent the major classes of water constituents, which are optically active, i.e. which have an influence on the underwater light field and RLw.

The advantage of the NN technique are:

- It represents a complex radiance model, which could not be used directly for the evaluation of remote sensing data due to its high computational demand.

- Since the model can be a radiance model it is not necessary to parametrize the conversion between different directions and the relationship between irradiance reflectance and radiances.

- In principle it is possible to set up a library of different NNs, where each NN is dedicated to the properties of a certain coastal area and is selected by the processor accordingly.

- The variability of the optical components as well as the expected uncertainties in the water leaving radiance reflectance spectra (after atmospheric correction) can be included in the training data set so that the NN learns these uncertainties and variability.

- For mass production it is fast and does not contain any iterations

Disadvantage is the higher demand for producing the training and test data set and for training the NN. However, by using a Linux-clusters this demand in no longer a significant problem.

The most critical step, as for any case 2 water algorithm, is the set up of the bio-optical model. It requires

(1) the consideration of how many components are necessary to describe the variability of the water leaving radiance reflectance spectra (RLw(λ),

(2) the determination of the inherent optical properties (absorption and scattering) of these components,

(3) the variability of these IOPs for each component,

(4) the range of each IOP to include most of the coastal areas and

(5) the relationship between the IOPs and the concentrations of the water constituents, which represent the IOPs.

Thus the development of the NN algorithm as developed for OLCI consists of the following steps:

- Collection of IOP and concentration measurements from different areas

- Determination of the number of independent components from the set of step 1

- Determination of the variability of each component, their ranges and, if possible, covariance

- Determination of the relationship between each component and different water constitutes

- Set up of the bio-optical model

- Simulation of a set of directional water leaving radiance reflectances, which cover the range of each component and different sun zenith angles

- Design and Training of the neural network

The NN can be delivered in the form of a subroutine or a look-up table. In case of a look-up table the NN coefficients are used by a NN processor, which is implemented in the overall processor in the form of a subroutine.
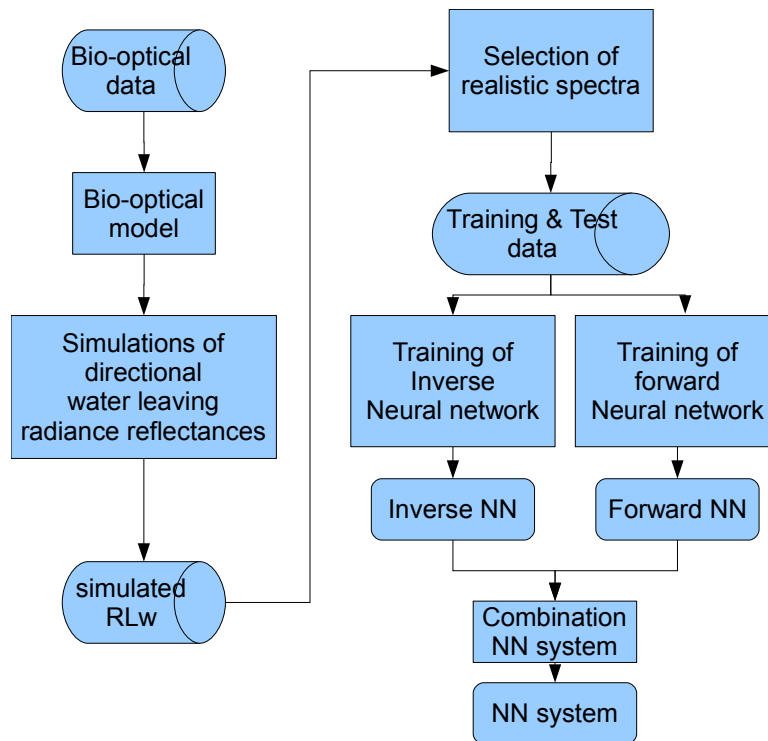
Fig. 1: Overview about steps to create the NN algorithm

3 ALGORITHM DESCRIPTION

3.1 Theoretical Description

The theory comprises three parts: (1) the bio-optical model, (2) the simulation of the water leaving radiance reflectances, (3) design and training of the neural network

3.1.1 Selection of spectral bands

All simulations are performed for the center wavelengths of the following 15 spectral bands of OLCI:

400 412.5 442.5 490 510 560 620 665 673.75 681.25 708.75 753.75 778.75 865 1020 nm

for the training of the water neural network the following 10 bands are used:

400 412.5 442.5 490 510 560 620 665 673.75 708.75 nm

3.1.2 Bio-optical model

The bio-optical model is based on pure water and 5 variable components:

- absorption by particulate organic matter / humic acids

- absorption by dissolved organic matter / fulvic acids

- absorption by phytoplankton pigments

- scattering by total suspended matter

- scattering by white particles

The idea is that these components and mixtures of them are able to represent most of the standard optical properties of case 2 waters. However, special cases such as exceptional blooms (red tides, blooms of cyanobacteria etc.) are not included; they need a special treatment (s. below).

For these components (except for white particles) a certain range of variability is assumed. This range is expressed in the form of a variable spectral exponent, which is varied randomly for each case in the simulation of the water leaving radiance reflectance according to a Gaussian distribution. For the phytoplankton pigment component a set of 221 different spectra have been compiled from measurements in the North Sea, Skagerrak and Norwegian Sea from different seasons. For the simulation of the RLw one of these absorption spectrum is selected randomly for each case.

In the set up of the bio-optical model, no co-variances between the components are defined. These are later determined implicitly by selecting the spectra for the training of the NN from the overall set of simulated reflectance spectra (s. below).

3.1.2.1 Pure water absorption and scattering

Pure water absorption data for the spectral range 400 - 900 nm are taken from the STSE Water Radiance Project (ESA Contract STSE- AO 1-5859/08/NL/CT). The absorption properties are complied from data of Pope & Fry (1997), Zheng & Fry (2005), for the NIR part of the spectrum > 900 nm from Hale & Querry (1973). The effect of temperature and salinity on the absorption coefficients with its uncertainties are take from Roettgers & Doerffer (2007) and Roettgers (unpublished).

The scattering spectrum is computed according to Zhang et al. 2009, Zhang & Hu 2009. This model takes also temperature and salinity effects into account, which have a significant influence for waters with low turbidity.

3.1.2.2 Yellow matter absorption

To describe the absorption by carbon-related matter two components with different spectral exponents have been defined (1) *humic acid* and (2) *fulvic acid*.

The component *humic acid*, with a spectral exponent of 0.008, is assumed to describe the absorption by humic acids and the absorption by suspended matter after bleaching of the

pigments in the sample. This fraction consists mainly of particulate and dissolved carbon of allochtonic origin, i.e. matter which is transported by rivers into the coastal sea.

The component *fulvic acid* decribes fulvic acids and all coloured dissolved organic matter (CDOM), which are mainly of autochtonic origin, i. e. products of the metabolisms of marine organisms.

The fractions of each component of the sum of both components should then describe the nature of yellow matter in the water.

The absorption spectrum is described as:

$$a_y(\lambda) = a_y(443\text{nm})\exp(-\epsilon_y(\lambda - 443\,nm))$$

where ϵ_y is the spectral exponent, which is 0.008 in the case of humic acids and 0.022 in the case of the fulvic acid component. Both components are varied with a standard deviation of 0.002.
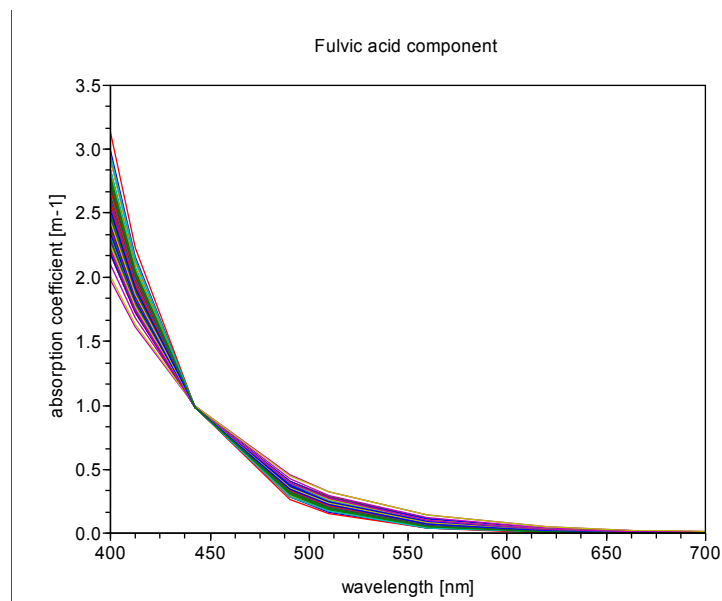
Fig. 2: Absorption variability of "fulvic acid" component
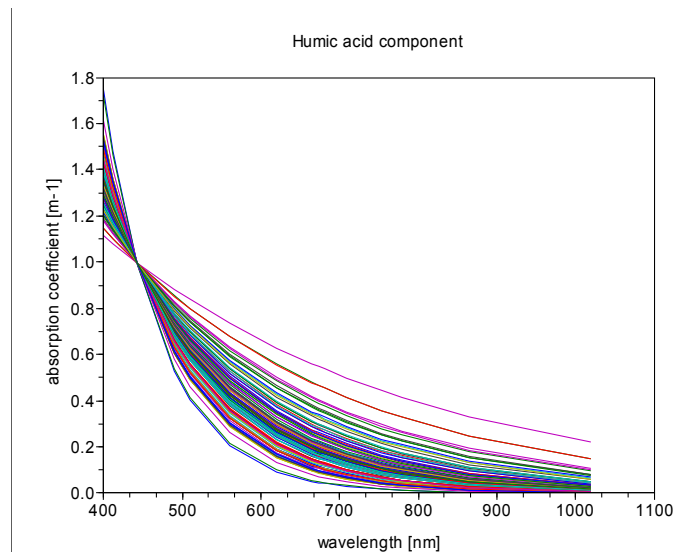
Fig. 3: Absorption variability of "humic acid" component

3.1.2.3 Absorption by phytoplankton pigments

The absorption by phytoplankton pigments are represented by 221 different absorption spectra which have been measured by using the filter pad method. The water samples have been collected in the North Sea, Skagerrak and Norwegian Sea by GKSS and NIVA in the framework of the EU funded projects COLORS and REVAMP during spring through autumn season. The spectra were normalized at 443 nm. For the final training additional data will be used, which will be compiled during the CoasColour Project of ESA.
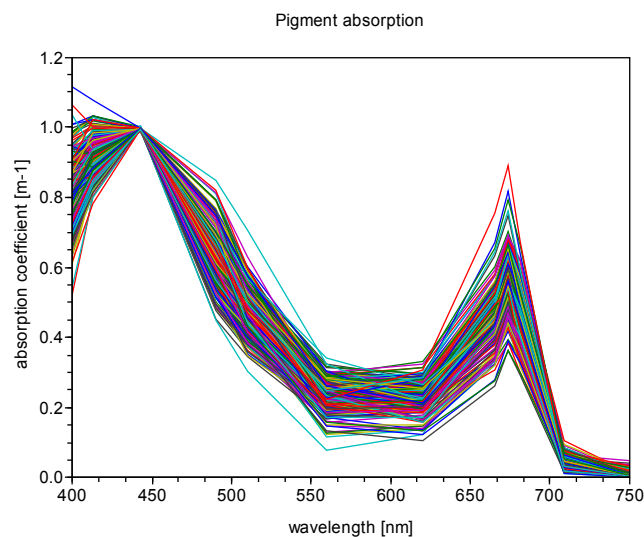
Fig. 4: Absorption variability of phytoplankton pigment

3.1.2.4 Suspended Matter

The spectral scattering coefficients of suspended particles in the water (including the scattering properties of phytoplankton) are described by

$$b_p(\lambda) = (\lambda/443\text{nm})^{(-\epsilon_p)}$$

with ϵ_p the spectral exponent, which was set to 0.8 with a standard deviation of 0.2.
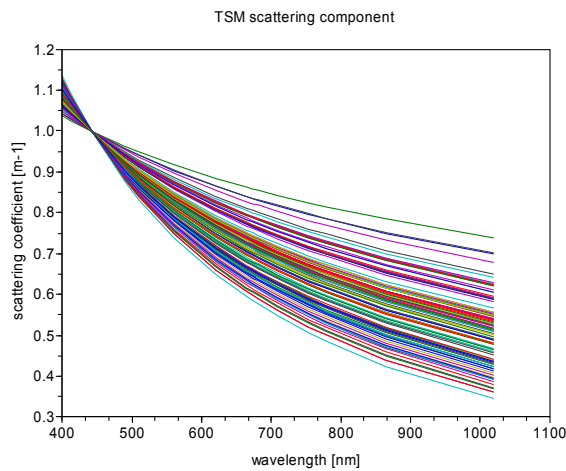
Fig. 5: Scattering variability of total suspended matter

3.1.2.5 White particle scattering

The white particle component represents mainly coccolithophorides and bubbles /foam in the water. A high value without high wind (s. auxiliary data) is an indicator of the presence of coccolithophorides. Also the contribution by bubbles to the optical properties of the water are captured by this component.

The component is described by a constant scattering coefficient of unity for all spectral bands.

3.1.2.6 Range and frequency distribution

For the simulation of the data set of reflectances for training of the NN a large number of different cases have to used to represent most of the natural waters. This number must cover the range between the minimum and maximum values of each IOP component, which are generally observed in the sea and coastal waters. Furthermore, one has to select the IOPs for the calculation of each spectrum from a frequency distribution, which is sufficiently dense. Significant holes in the distribution would reduce the interpolation capability of the neural network. If one assumes 3 orders of magnitude for each component, and 5 steps per

magnitude it would be necessary to simulated 15^5 = 759 375 Spectra, which would require > 1 month computation time on a Linux cluster with 16 nodes. Thus it is necessary to reduce this number significantly by sampling the IOPs from a random distribution.

Initially all components are defined as independent from each other. Later the covariance between the components is implicitly introduced by the selection of the water leaving radiance reflectance spectra (s. chapter 3.1.4).

First the total scattering and total absorption coefficients for $\lambda = 443\,nm$ are selected randomly from a logarithmic scale. This is to avoid a Gaussian distribution of the overall scattering and absorption coefficients and, thus, a bias in the data, which would be the result if all components are varied independently by using a uniformly distributed random number over the full scale,

In a next step the value is distributed randomly between the 3 absorption or 2 scattering components respectively.

The code for this procedure is as follows:

$$atot = exp(log\_atot\_an + ran1() * (log\_atot\_en - log\_atot\_an)),$$

$$btot = exp(log\_btot\_an + ran1() * (log\_btot\_en - log\_btot\_an)),$$

where *log_atot_an* is the logarithm of the maximum and *log_atot_an* of the the minimum absorption coefficient at 443 nm. *ran1* is a uniformly distributed random number.

In the next step *atot* and *btot* are distributed among the absorption or scattering components. as follows:

```
// for the 3 absorption components
    acase=ran1(idumrand)*3
    arest=atot
    if (acase .lt. 1.0) then
       conc_agelb=ran1()*arest
       arest=arest-conc_agelb
       conc_apart=ran1()*arest
       arest=arest-conc_apart
       conc_apig=arest
    elseif (acase .lt. 2.0) then
       conc_apart=ran1()*arest
       arest=arest-conc_apart
```

```
        conc_apig=ran1()*arest

        arest=arest-conc_apig

        conc_agelb=arest

    elseif (acase .lt. 3.0) then

        conc_apig=ran1()*arest

        arest=arest-conc_apig

        conc_agelb=ran1()*arest

        arest=arest-conc_agelb

        conc_apart=arest

    endif


// for the 2 scattering components

    acase=ran1()*2

    brest=btot

    if (acase .lt. 1.0) then

        conc_bpart=ran1()*brest

        conc_bwit=brest-conc_bpart

    else

        conc_bwit=ran1()*brest

        conc_bpart=brest-conc_bwit

    endif
```

Scatter plot and histograms of the frequency distributions of the optical properties are given in figures 6 - 14.
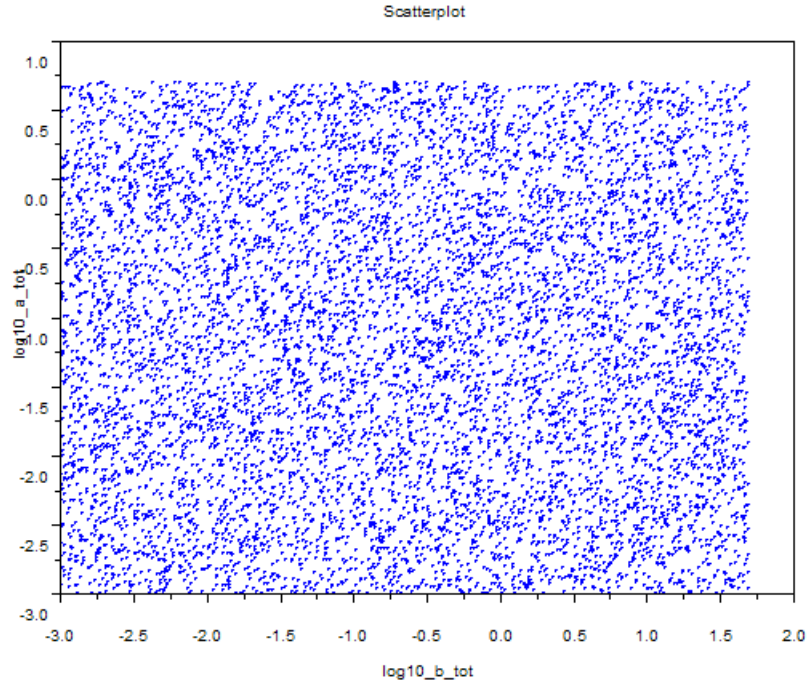
Fig. 6: Scatter plot of total scattering and total absorption of all water constituents
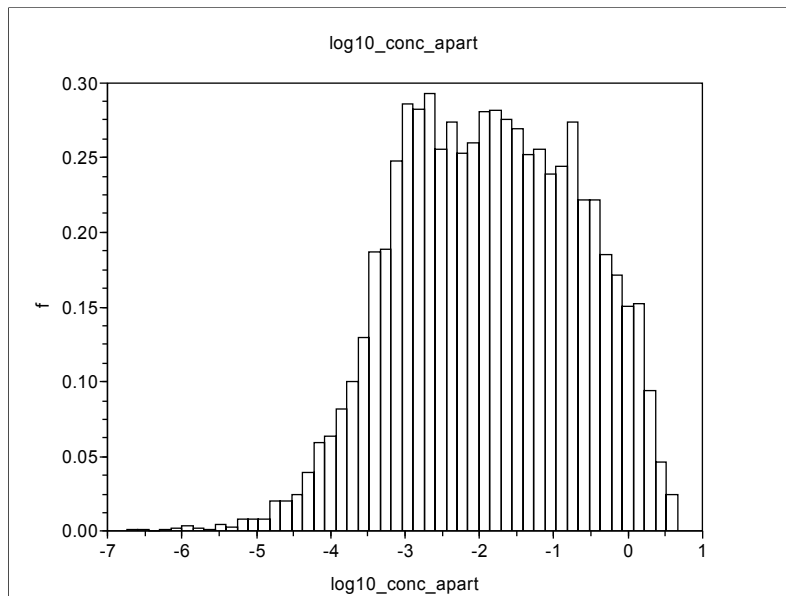
Fig. 7: Frequency distribution of "humic acid" component / particle absorption
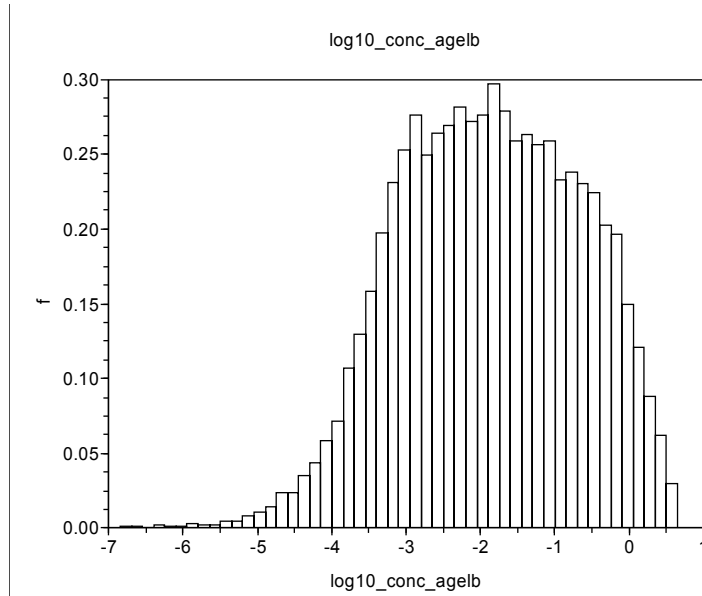
Fig. 8: Frequency distribution of "fulvic acid" component absorption at 443 nm
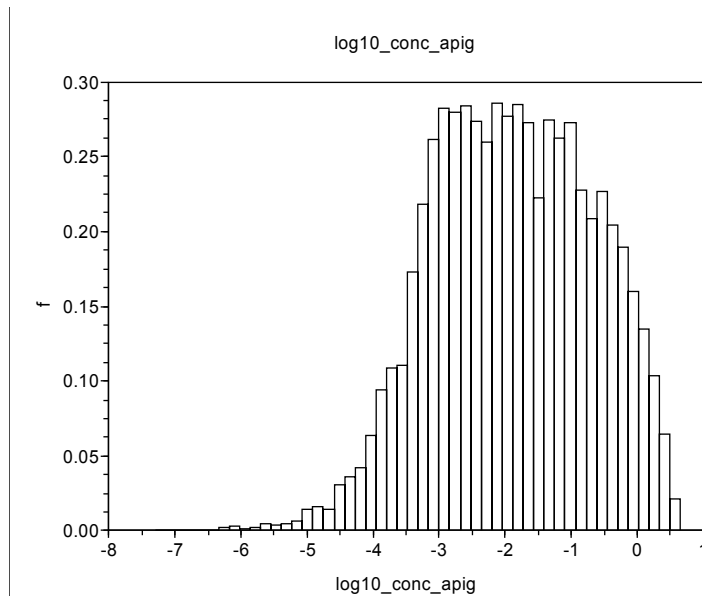
Fig. 9: Frequency distribution of pigment absorption at 443 nm

log10_conc_bpart
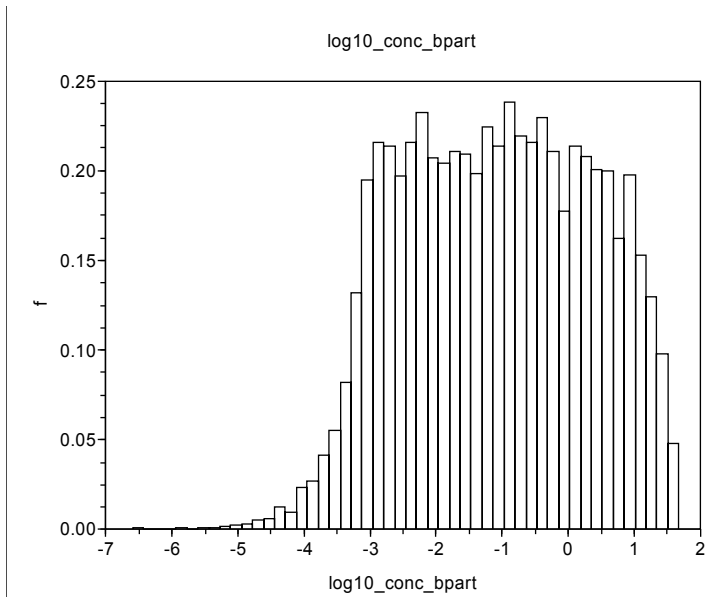
Fig. 10: Frequency distribution of total suspended matter scattering at 443 nm

log10_conc_bwit
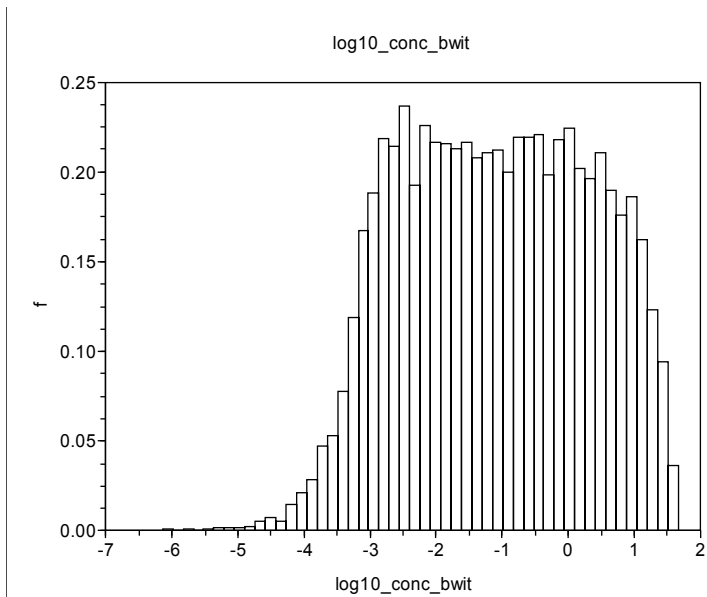
Fig. 11: Frequency distribution of white particle scattering
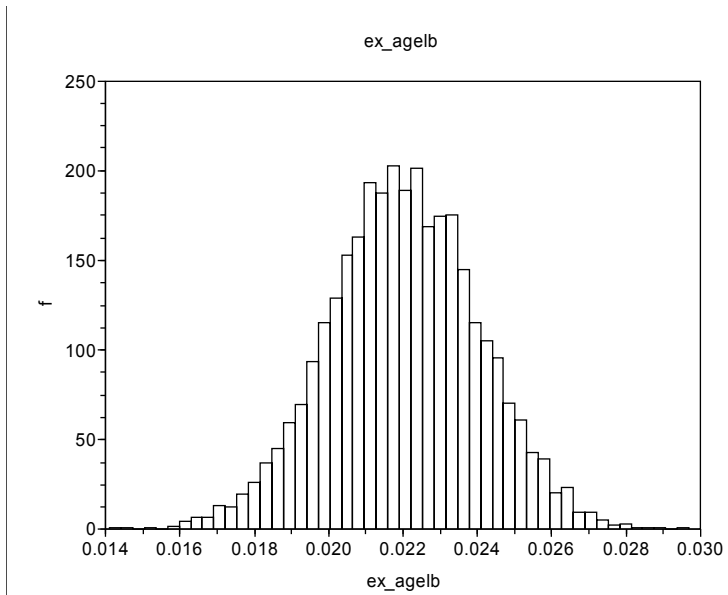
Fig. 12: Frequency distribution of the spectral exponent for "fulvic acid" component
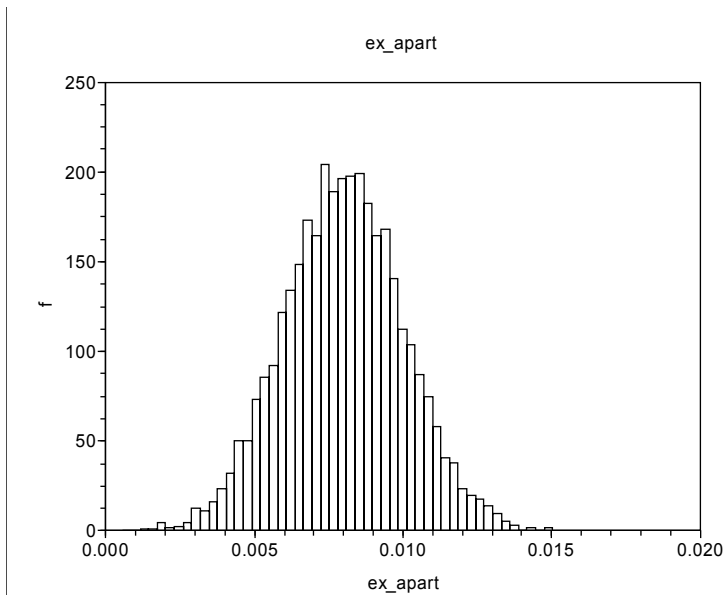
Fig. 13: Frequency distribution of the spectral exponent for "humic acid" component
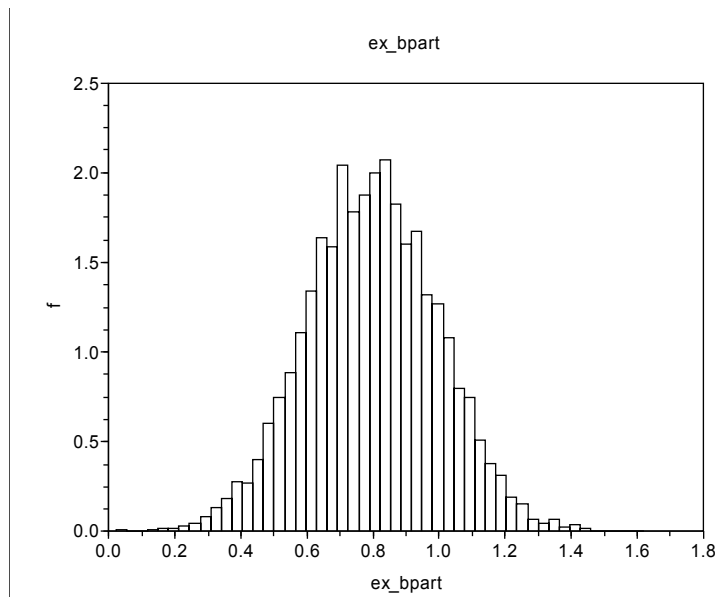
Fig. 14: Frequency distribution of the spectral exponent for particle scattering

3.1.3 Simulation of the radiance reflectance spectra

The simulations are performed with Hydrolight (Mobley, 1994), which has been extended for the production of a large number of RLws for training and testing of the NN.

The downwelling radiance distribution just above the surface is also calculated with Hydrolight, which is used in this case to simulate the radiative transfer in the atmosphere. A standard atmosphere according to reference model for MERIS is defined with a rough sea surface corresponding to a wind speed of 3 m/s. The radiance distribution is calculated for 36x24 quads (azimuth and zenith angles) for 17 sun zenith angles for all of the selected 15 spectral bands of OLCI.

One of these 17 different skies is randomly selected for each case of the simulation run and then used as input for the water radiance simulations.

The radiance distribution of the water leaving radiance, $RLw(\lambda, \theta, \phi)$, is calculated for the same directions as the incoming radiance also for all of the selected 15 spectral bands.

It is assumed that the vertical distribution of all components is homogeneous and that the optical depth of the water is infinite, i.e. no bottom effects are assumed.

From each simulation case 7 different radiances are selected randomly from the 36x24 angles with a uniform random number distribution so that the number of training cases increases by the factor of 7.

3.1.4 Selection of spectra for the training of the neural networks

A subset of all simulated RLw were selected to use only those spectra, which are in the range of measured spectra. Measurements in North Sea by GKSS, in particular in the German Bight, and data of measurements, which are stored in the MERMAID data base, was used to determine lower and upper reflectances for some spectral bands as selection criteria.

These limits are listed in Table 1.

OLCI band	wavelength nm	RLw min sr-1	RLw max sr-1
2	412	0.001	0.016
3	490	0.0017	0.015
4	510	0.0017	0.017
5	560	0.0008	0.022
11	708	0.0	0.017
16	865	0.0	0.0045

Table 1: Restriction of RLw for some spectral bands for selection of realistic spectra

The consequence of this selection is that the underlying IOPs, which determine the RLw are constrained. Furthermore, covariances occur, when comparing the frequency distribution of the IOPs after the selection. The histograms and scatter plots are shown in the following figures 15 - 17. The resulting co-variance is listed in Table 2.
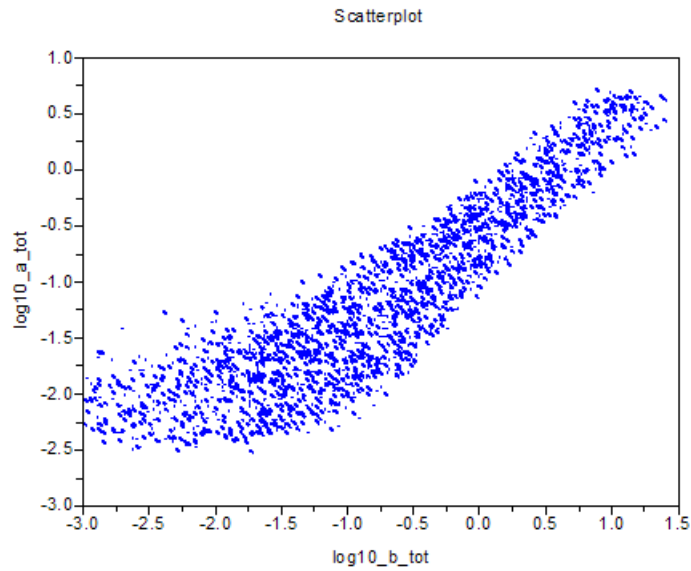
Fig. 15: Scatterplot total scattering vs. total absorption after selection of realistic reflectance spectra
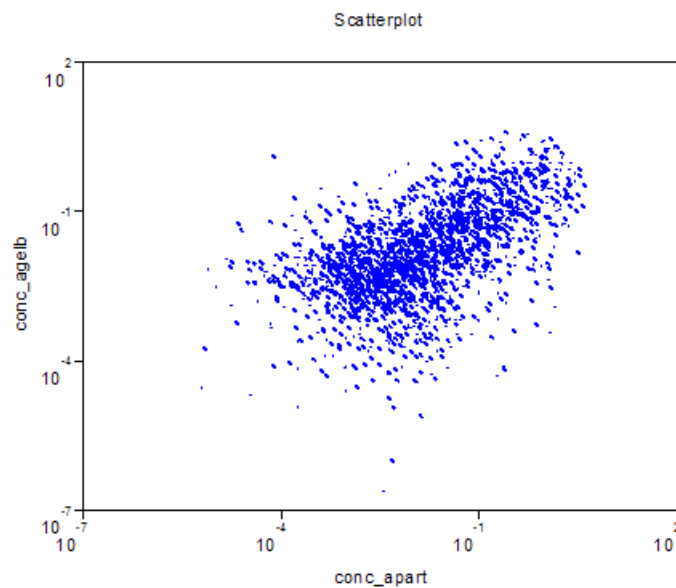
Fig. 16: Scatterplot absorption of "humic acid" component (x-axis) vs. "fulvic acid" component
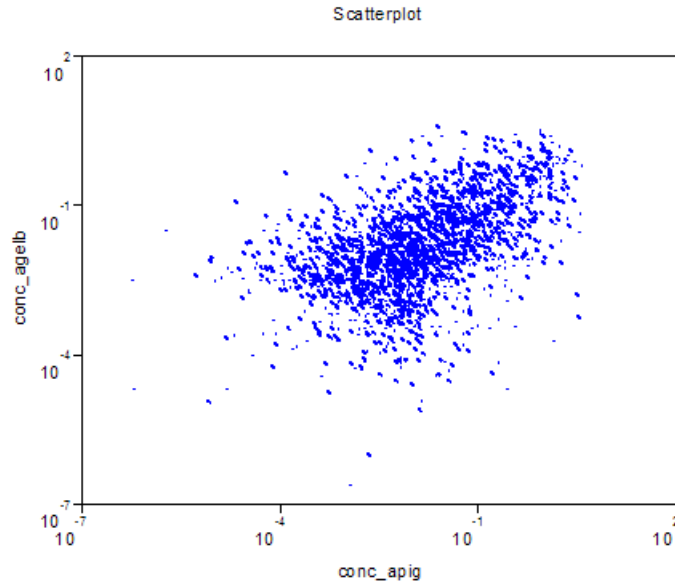
Fig. 17: Scatterplot absorption of pigment absorption (x-axis) vs. "fulvic acid" component absorption

	a_pig	a_fulvic	a_humic	b_part	b_wit
a_pig	1	0.503	0.626	0.748	0.729
a_fulvic		1	0.510	0.612	0.609
a_humic			1	0.755	0.752
b_part				1	0.842
b_wit					1

Table 2: Korrelations between the log of the IOP components after the selection

3.1.5 Design of the neural network system

The NN-system consists of 2 NNs, an inverse network and a forward network. The inverse NN is used to determine the IOPs from the measured RLws (after atmospheric correction). The forward NN is used to test if the input RLw spectrum is in agreement with the spectra, which are included in the training data set, i.e. if the measured RLw is in scope of the NN.

3.1.5.1 Inverse NN

The inverse NN, which have been trained for this ATBD and the corresponding sensitivity study (45x20x15x8_107.1.net) has 15 input neurons, 4 hidden layers with 45, 20, 15 and 8 neurons and 5 output neurons. Input are the log10 RLws of OLCI bands 1-9 and 11, temperature and salinity and 3 angles, the sun zenith, the viewing nadir and the azimuth difference between sun and viewing direction. That means that the NN is trained with directional radiances, not with the normalized angles of irradiance reflectances. So no conversion functions are necessary as it is the case if the simulations would be based on irradiance or normalized remote sensing reflectances. Output are the 5 IOP components, i.e. absorption coefficients of (1) humic acids / bleached particle absorption, (2) fulvic acid, (3) pigment absorption and the two scattering coefficients of (4) scattering of total suspended matter and (5) of white particles. All output values are the log10 values for OLCI band 3 (443 nm).

3.1.5.2 Forward NN

The corresponding forward NN (45x20x15_32.9.net) has 10 input neurons, 3 hidden layers with 45, 20 and 15 neurons, and 11 output neurons. The input neurons are the log10 values of the 5 IOP components, water temperature and salinity and the three angles as described above; the output neurons are the log10 RLws for the first 11 MERIS bands. However, band 10 is the RLw without the solar stimulated fluorescence of phytoplankton chlorophyll, since the fluoresce is not included in the simulation.

3.1.5.3 Combination of inverse and forward NN to determine the out of scope distance

The output of the inverse NN is used as input to the forward NN. Its output, i.e. the RLws of OLCI bands 1-9 and 11, are compared with the measured RLw spectrum according to

$$\chi^2 = \sum_{i=1}^{i=n} \left((RLw_m(i) - RLw_s(i))^2 / n \right)$$

with $RLw_m(i)$ the measured radiance reflectance for OLCI band i and $RLw_s(i)$ the corresponding simulated spectrum of the forward NN. χ^2 is then a measure of how far the input spectrum is out of the scope of the training data set. It can be used as an *out of scope* indicator product on a pixel-by-pixel bases or, as it is the case for MERIS, but with less information, to trigger a flag if χ^2 is above a certain threshold, which has to be defined.
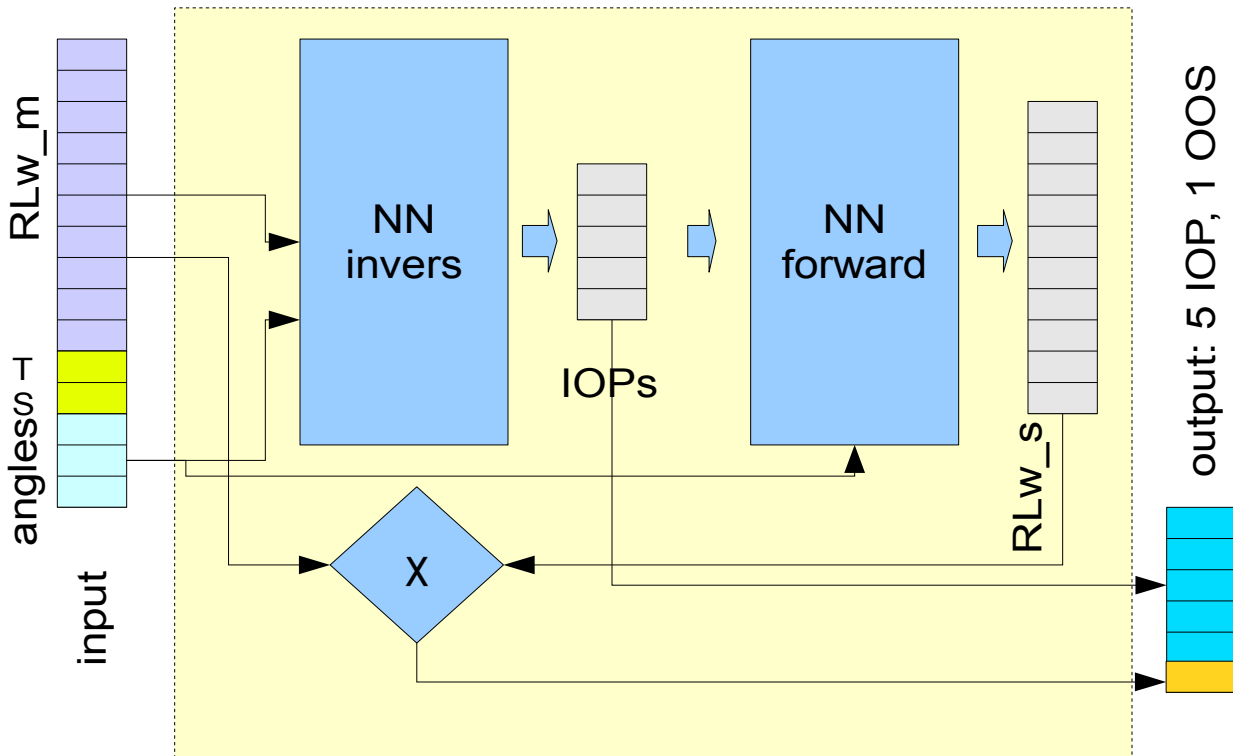
Fig. 18: The neural network system as proposed for OLCI

3.1.5.4 Cut-off reflectance

The water leaving radiance can be very low so that the RLw, which are computed from TOA radiance after atmospheric correction, can become uncertain or even negative. This is the case for the red spectral bands in case 1 waters or for the blue bands in waters with high concentrations of phytoplankton and in particular of yellow substances (humic acids). RLws with high uncertainty of even negative RLw would have a strong negative impact on the inverse neural network. Thus a threshold is defined for all RLw. Whenever a RLw is less than this threshold the the threshold value is used as RLw. This requires that the NN is trained with the same threshold.

This feature has been included in the standard case 2 water NN for MERIS.

3.1.6 Conversion of the IOPs into concentrations

Since most users are more interested in concentrations than in IOPs, functions are included in the case2 water processing part, which convert the IOPs into concentrations of chlorophyll a (chla) and total suspended matter dry weight (TSM) on the bases of empirical relationships.

In agreement with the MERIS processor the following functions are preliminary proposed:

$$\text{chla [mg m-3]} = 22 * a\_pig(443) \verb|^|1.04$$

$$TSM = 1.7 * b\_part(443)$$

3.1.7 Optional modifications and extensions

A number of extensions to the proposed procedure are possible, which partly have been realized already for MERIS in the Case2R processor of the BEAM software.

3.1.7.1 Calculation of the total absorption and scattering coefficients

These products can be simply computed by adding the different components:

a_tot = a_pig + a_humic + a_fulvic

b_tot = b_part + b_white

It has been demonstrated (IOCCG report 5) that total a and total b are much more robust against errors than the IOP components. Thus, they are more appropriate to build up climatological data records.

However, these computation can be easily performed in the BEAM processor without generating these product in the IPF.

3.1.7.2 Calculation of the light penetration depth /transparency

The wavelength with maximum light penetration in water changes with increasing concentration of water constituents from around 440 nm to longer wavelengths up to the green - red spectral range. This spectral shift and the penetration depth can be computed by using the bio-optical model, which is the basis for the neural network. The computation of the the spectral attenuation coefficients for the downwelling irradiance, $k_d(\lambda)$, can be included in the Hydrolight simulations and be used to determine e.g. the signal depth z_{90} for the 3 OLCI bands with minimum k_d coefficients, which is closely related to the secchi disc depth. A further possibility is to compute the 90% attenuation depth as the mean from the k values of the three OLCI bands with minimum k. These relationships can be converted into a special NN or included in the basic inverse NN.

This calculation is included in the C2R processor of BEAM.

3.1.7.3 Calculation of the confidence / uncertainty range

The products (IOPs, concentrations) derived from RLws have always an uncertainty or confidence range, which may vary from pixel to pixel. As an example the confidence range for a chlorophyll *a* value is much smaller, when all other components are low in contrast to the case when one or all other components have high values. E. g. a high concentration of suspended matter can easily mask the effect of a small chlorophyll concentration on RLw.

This confidence range can be computed on a pixel by pixel basis. It would be of high importance for users so that they can decide whether the accuracy of a pixel value is acceptable for his purpose.

3.1.7.4 Identification of exceptional plankton blooms and computation of a bloom index

Whenever the χ^2 value indicates an out of scope spectrum for a pixel the cause might be an exceptional plankton bloom. This can be tested by comparing the spectrum with a number of bloom spectra, which are included in a library, using a fast Chebychev criteria. A suitable NN, which was trained for such a bloom can than be selected and applied according to the result of this test.

3.1.7.5 Inclusion of the atmospheric correction for case 2 water

Since the atmospheric correction (AC) is extremely critical for case 2 water remote sensing a special AC correction also based on a neural network could be included in the case 2 water processing part. In this case the input would be directly the directional top of atmosphere radiance reflectances. The performance of such an approach has been demonstrated already with the AC included in the C2R processor of BEAM. Since such a branch was not foreseen up to now, we propose to implement it with a switch so that the decision if this AC branch shall be used permanently as input to the NN based water retrieval prodedurte can be decided after some first tests without modification of the code (s. also chapter 6.2).

Justification for this proposal is the fact that the standard atmospheric correction procedure is adapted to clear ocean case 1 water. By including a special bright pixel algorithm it can also be applied to bright turbid water. However, since the algorithm is based on spectral bands in the near infrared spectral range from the reflectance of which the atmospheric properties are derived, it requires an extrapolation to the green-blue spectrum. This extrapolation is extremely critical in particular in waters with high concentrations of absorbing constituents (organic matter, phytoplankton) where the water leaving reflectance can be less than 5% of the reflectance at top of atmosphere. The experience with MERIS has demonstrated that many pixels have to be flagged in case 2 water due to the fact that the atmospheric correction has produced incorrect and negative water reflectance spectra.

The proposed alternative atmospheric correction procedure uses the full TOA reflectance spectrum and excludes by its mechanism negative reflectances. Furthermore, it is able to correct sun glint contaminated areas so that in total many more pixels in case 2 waters can be processed to useful products than with the case 1 water atmospheric correction procedure.

Details are desribed in the corresponding ATBD for OLCI.

	SENTINEL-3 L2 PRODUCTS AND ALGORITHM DEFINITION OLCI L2 ATBD Ocean Colour Turbid Water	Document Ref: S3-L2-SD-03-C11-GKSS-ATBD Issue: 2.1 Date: 20100715 Page 29 of 50

GKSS FORSCHUNGSZENTRUM in der HELMHOLTZ-GEMEINSCHAFT

3.1.7.6 Expected modifications after completion of the "water radiance" project

Presently a consortium of laboratories is at the beginning of the project "water radiance" under ESA contract. Goal of this project is to analyze advances in ocean optics, in particular in measurements of IOPs of pure water and its constituents, establish a new bio-optical and water radiance model, and develop or modify algorithms for OLCI. It is expected that the results of this project will also be utilized to update the standard case 2 water algorithm for OLCI, such as described in this ATBD.

3.2 Practical consideration

As it is the case for MERIS the NN system can be provided in the form of a look-up table. In this case the processor must include a function or subroutine which reads the coefficients and sets up the NN structure and functions from the parameters of this look-up table.

A more flexible alternative would be a plug-in structure, where the case 2 water processing part including the NN would be delivered in the form of a subroutine, which must either be included into the compilation or linked to the processor in the form of a dynamical link library (dll).

4 ASSUMPTIONS AND LIMITATIONS

The algorithm in the presently proposed form includes the following assumptions and limitations:

- The NN algorithm is only valid for the IOP components and the ranges of the IOPs as defined in the bio-optical model.

- The uncertainty for each IOP component increases with decreasing concentration of the substances, which determines that IOP and with increasing concentrations of the substances, which determine all other IOP components. Thus, the accuracy may vary from pixel to pixel and can surmount even an 100% error. However, this is due to the nature of the problem and is independent from the art of the algorithm.

- The model assumes a vertical homogeneously distribution of all components

- The model assumes an infinite water depth, i.e. no bottom reflection effects

- The model neglects any inelastic scattering (Raman scattering, fluorescence)

5 ERROR BUDGET

The retrieval error as treated in the algorithm is determined by two causes:

(1) the input spectrum to the NN is out of scope of the data set, which was used for training of the NN. This can be due to various causes: by various errors of the instrument or the atmospheric correction, by the optical properties of a water substance or a phytoplankton

population, which was not included in the bio-optical model used for training of the NN, by bottom reflection or stratification in water. This type of error is captured by the combination of a backward and forward NN as described in chapter 3.1.5.3. Output of the procedure is the deviation between the input spectrum and the spectra produced by the forwardNN. This can used as a quality indicator and/or to trigger a warning flag.

(2) Another error is due to the ambiguity range, which is caused either by the non-linear relationship between concentration and reflection at the higher concentration range, where the effect levels of, or by an other but dominating component, For example: the contribution of chlorophyll to the reflectance may be small in the presence of high concentrations of yellow substances or suspended matter, while the same concentration might have a significant effect on reflectance in cases where the concentrations of the other components are low (s. Fig. 19. The consequence is that the uncertainty range for each component may vary from pixel to pixel.
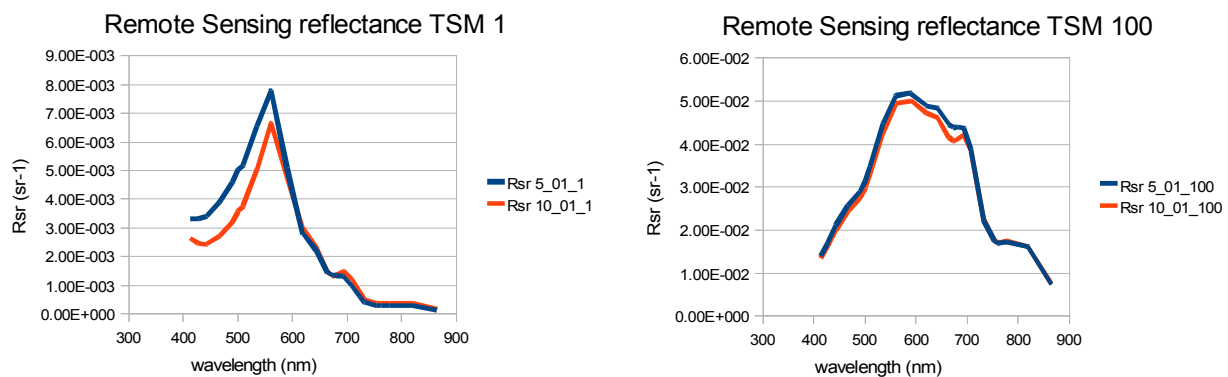

Fig. 19: Water leaving radiance reflectance spectrum for 5 and 10 mg m^{-3} of chlorophyll and an absorption by yellow substance of 01 m^{-1} at 443 nm. left: Total suspended matter concentration of 1 g m^{-3}, right of 100 g m^{-3}

These effects on the uncertainty require an uncertainty map for each component.

There are two alternative ways to compute these uncertainty maps. It can be computed from the Hessian matrix for each pixel by using the forwardNN within an iteration using an optimization technique. This version has been implemented in the C2R processor, which has been developed for the BEAM processor. The other option is to pre-calculate the errors with the same technique for the scope of the processor and train a special neural network. This version will be much faster for mass production runs and is recommended here. This would extend the processor as indicated in Fig. 20.
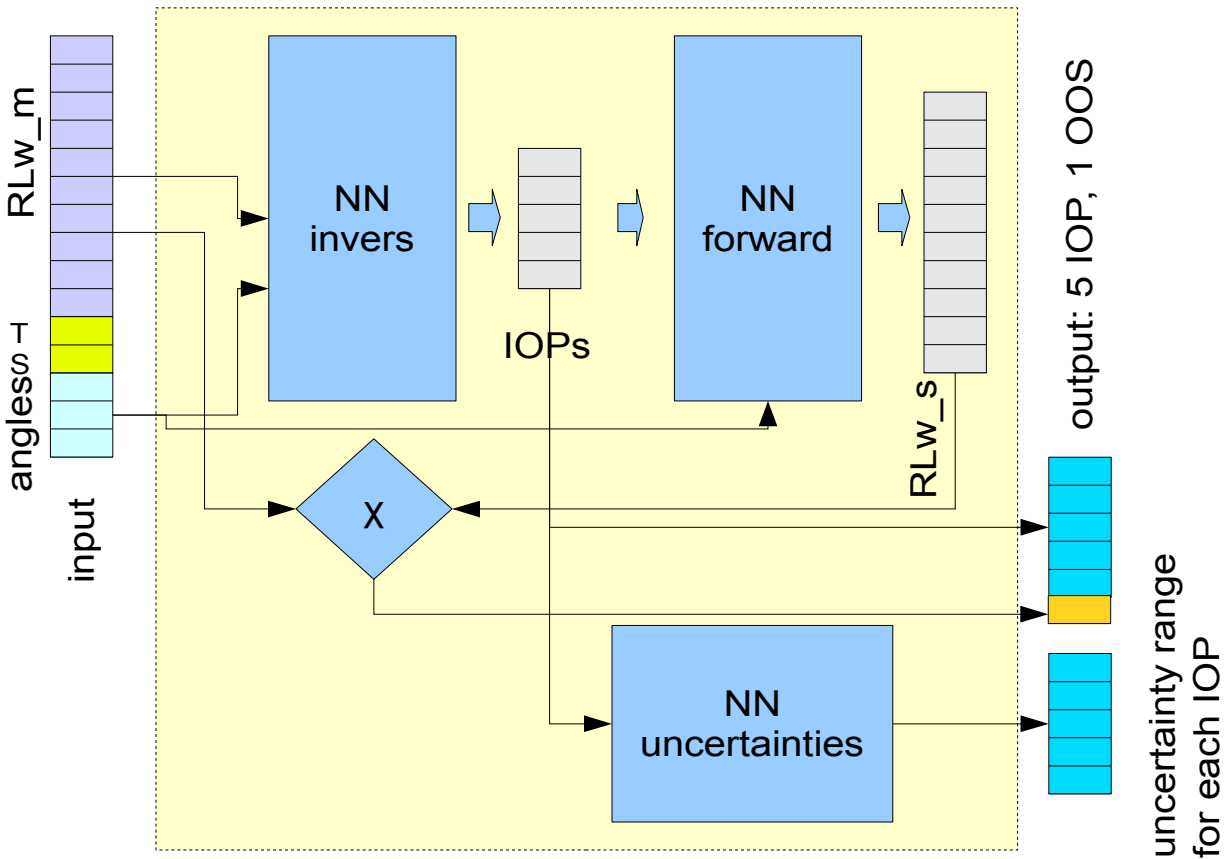
Fig. 20: Extension of the NN processor with a NN to compute the uncertainty range for each component

6 INPUT DATA

There are two options.

(1) input of water leaving radiance reflectances RLw after the atmospheric correction.

(2) Input from TOA radiance reflectances

6.1 Input of RLw

In this case input to the Neural network are:

1-9: the directional water leaving radiance reflectances $RLw(\lambda, \theta, \phi)$ [sr⁻¹] of the OLCI bands O1 - O8, O10,

10: solar zenith angle (degree),

11: view zenith angle (degree),

12: difference between solar and viewing azimuth angle (degree).

13: water temperature

14: salinity

This version requires an accurate atmospheric correction for all 9 bands, which are used for the NN, i.e. for the entire spectral range 400 - 708 nm for all case 1 ancd case 2 water conditions.

6.2   Input of RLtoa

In this case the procedure has to be extended by the atmospheric correction as implemented in the BEAM C2R processor. This AC processor is based on a a reconstruction of RLw for all bands from RLtoa by a neural network rather than by an extrapolation technique from reflectances in the NIR bands, which leads to errors in particular at low reflectances in the blue-green spectral range in case of high concentrations of absorbing material such as humic substances or phytoplankton.

In this case the procedure requires the following inputs:

1-15: RLtoa bands O1-O11, O14 (778 nm), O16 (865 nm), O18 (885 nm), O19 (900 nm)

16: solar zenith angle (degree),

17: view zenith angle (degree),

18: difference between solar and viewing azimuth angle (degree).

19: surface pressure (from aux data)

20: ozone (from aux data)

21: water temperature

22: salinity

Due to the problems with the standard atmospheric correction procedure over some types of case 2 waters it is strongly recommended to implement also this option in the way as presented in Fig. 21. The proposed switch allows to decide whether this branch will be used permanently as input to the NN based retrieval algorithm after first tests without a modification of the code.
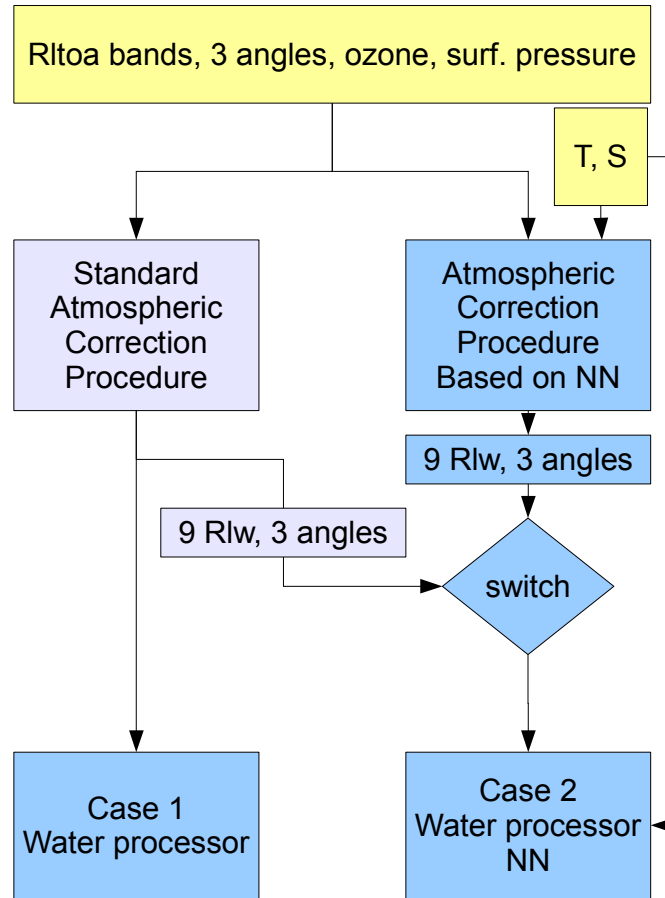
Fig. 21: Implementation of an optional alternative atmospheric correction for case 2 waters with a switch to decide about the input to the case 2 water NN after first tests.

7   OUTPUT DATA

7.1   Overview

Output products are related to the bio-optical model, which is used for the simulation of the training data set, which in turn is used for training of the neural networks, and are extended by derived products. All these products can be provided as output product.

The model is based on 5 variable components of inherent optical properties:

- absorption by particulate organic matter / humic acids

- absorption by dissolved organic matter / fulvic acids

- absorption by phytoplankton pigments

- scattering by total suspended matter

- scattering by white particles

These 5 inherent optical properties are provided as output, all for the wavelength 443 nm.

- The total absorption and scattering coefficients of all water constituents are given for all spectral bands of OLCI in the range 400 - 710 nm.

- The phytoplankton absorption coefficient is converted into chlorophyll concentration [mg m^{-3}].

- The total scattering coefficient is converted into suspended matter concentration (dry weight g m^{-3}).

Further derived products are:

- Downwelling irradiance attenuation coefficients: $kd(\lambda)$, which includes kd490

- Transparency given as z90_max (signal depth)

- Heated layer depth z90_heat

Out of scope conditions and uncertainties

- General out of scope: the mean square root deviation between the input reflectance spectrum and the spectrum reconstructed with the forwardNN.

- Uncertainties for each product in %.

7.2 IOP products

The inherent optical properties can be used for a variety of applications: (1) to adapt own (regional or local) conversion factors for calculating concentrations of suspended matter, organic matter or chlorophyll, or primary production. The products are the scattering or absorption coefficients for each of the 5 IOP components for the wavelength 443 nm (OLCI band 3). However , since the spectral distribution for each component has been defined in the bio-optical model and is documented, the user can easily compute the IOPs also for the other spectral bands.

These 5 IOPs can describe most of the optical variability in case 2 water. The two components for dissolved and particulate organic matter stay for optical components with an absorption spectrum, which is characterized by an exponential decrease in absorption with increasing wavelength. The two exponents stay also for major compounds in water, humic acids, with a spectral exponent of 0.008, and for fulvic acids with a spectral exponent of 0.022.

The "white" scatterer component is related to blooms of Coccolithophorides, but also to foam and bubbles in the water.

Not all components can be included in the bio-optical model. In particular exceptional plankton blooms may discolour the water in various ways. In these cases special algorithms are required. To detect these cases the "out of scope" algorithm was included (s. chapter 7.5)

Furthermore, the total absorption and scattering coefficients (a_tot, b_tot), i.e. the sum of the coefficients of all water constituents, is provided for all OLCI bands in the range 400 - 710 nm. This is a robust product (s. recommendation IOCCG report No. 5), since it avoids splitting into different components. Thus, these coefficients can be used for long time series and climatological data records.

7.3 Concentrations

Two products in form of mass concentrations are provided: total suspended matter dry weight (TSM, g m^{-3}) and the chlorophyll concentration (mg m^{-3}) as a proxy for phytoplankton.

Both are computed using the corresponding IOP, i.e. b_tsm and a_pig.

These products are common products, which are used in many application, including e.g. for the assimilation into suspended matter transport models or primary production models.

7.4 AOP products

Apparent Optical Properties (AOP) products comprise the water reflectances and variables related to the water transparency. The computation of the water reflectances are output of the atmospheric correction and are described in the corresponding ATBD.

The basic variable, from which the transparency and the penetration depth of light are derived, is the spectral downwelling attenuation coefficient kd (m^{-1}). It describes the attenuation of the

downwelling irradiance Ed: kd = -log(Ed(z+1/Ed(z)) with z the water depth in meter. As an apparent optical property it values changes with the radiation geometry and thus depends on the concentration and optical properties of water constituents, the water depth and the downwelling radiance geometry at the water surface. Thus, kd will be computed for the first attenuation depth 1/kd for each wavelength. These values come from the radiative transfer simulation, which are used for training of the neural network, so that the concentrations and optical properties of water constituents and the radiance geometry has been taken implicitly into account.

Using the kd values (which include kd490) two further products are derived, z90_max and z90_heat.

z90_max is the depth (m) of the water body, from which 90% of the backscattered radiation at the surface stems from. It is computed as the mean from the 3 spectral bands with minimum kd values (1/kdmin).

z90_heat is the depth in which 90% of the solar energy at the surface is absorbed and, thus, is mainly converted into heat. This depth depends on the concentration of optically active components in the water, which are described by the IOPs. Also for this variable the spectral kd values of all spectral bands are taken into account. It is also an outcome of the radiative transfer calculations.

7.5   Out of scope conditions and uncertainties

Since a generic case 2 water algorithm - as presented here - cannot cover all conditions in optically complex waters with its large and changing variety of water constituents, it is important to detect conditions, which are out of scope of the algorithm. A reason can also be a failure in the atmospheric correction. These conditions are defined and described as the root mean square deviation between the input reflectance spectrum and the reflectance spectrum, which is reconstructed by the forward neural network.

The uncertainties for each IOP product is defined by the range around the derived value, which causes a change of 5% in the reflectance spectrum. This range depends on the concentrations of all other water constituents. Th decrease or increase in chlorophyll concentration, which causes a change of 5% in the reflectance spectrum will be much larger in water with a high concentration of suspended matter than in clear oceanic water. Thus, these values will be provided on a pixel-by-pixel basis. These uncertainties will be determined also from the simulated training data set (s. also chapter 5 and Fig. 19).

Additional uncertainties of the concentration variables (TSM, chlorophyll) come from the variability in the conversion factors. These are directly taken into account.

The uncertainties of the AOPS are also computed from the radiative transfer simulations assuming an uncertainty in reflectance of 5%.

8   VALIDATION

The performance of the case 2 water algorithm has been demonstrated for MERIS in various presentations by different members of the MVT and by members of the team of the Case 2 Regional project.

Some of the results will be summarized here in the form of examples. The validation of the alternative atmospheric correction procedure is included in the corresponding ATBD.

Note that validation in complex case 2 water is difficult, because the spatial distribution of water constituents can be very patchy with a high temporal variability so that match-up data, which allow a direct comparison between the data of a pixel and a sample, are very rare. Thus the validation must be based on a number of different indicators.

8.1   Comparison with in situ data along transects

The main transect, which was used for validation of the case 2 water algorithm is located between Cuxhaven and the island of Helgoland in the North Sea (German Bight). Here a Ferryboat has been used as a platform for optical measurements and sampling whenever appropriate weather conditions and an ENVISAT overpass was predicted. Along this transect a strong gradient in all three components can be observed and used for validation.
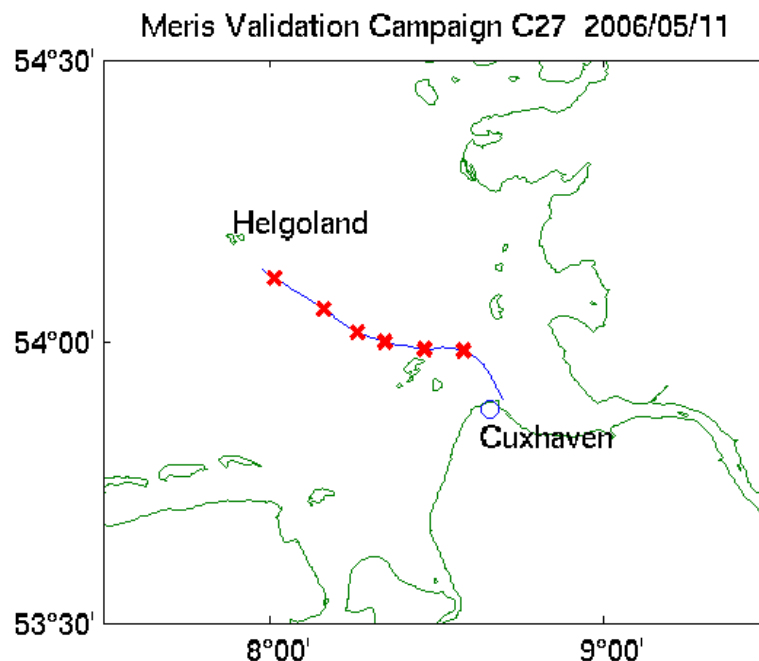

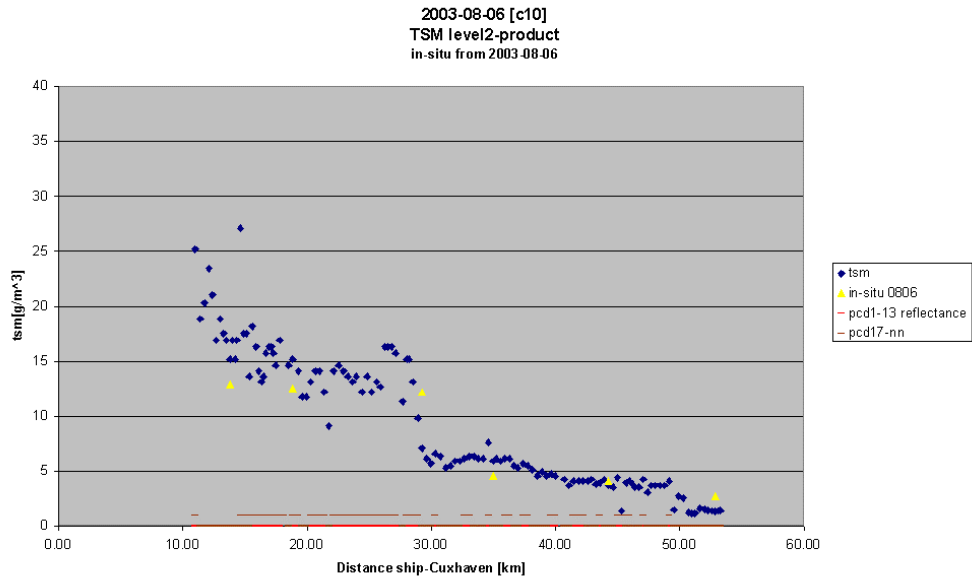*Fig. 22: Helgoland transect used for validation with sampling positions*

Fig. 23: Helgoland transect: Total Suspended Matter derived from MERIS (blue dots) and in situ data (yellow dots)
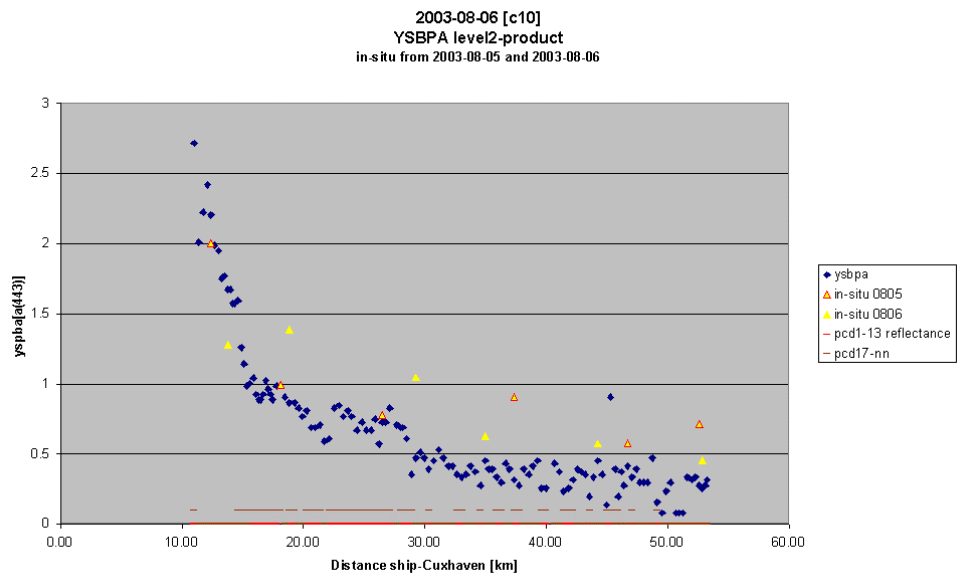

Fig. 24: Helgoland transect yellow substance derived from MERIS (blue dots) and in situ data (yellow dots).
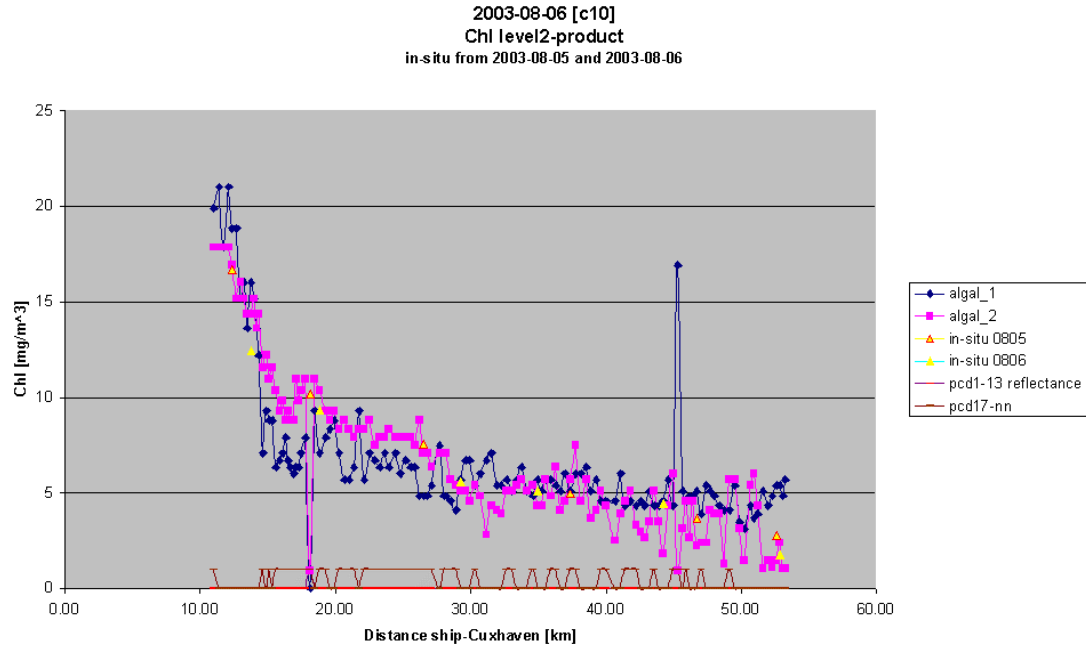
Fig. 25: Chlorophyll along Helgoland transect derived from MERIS and in situ samples: alsal_1 blue dots, algal_2 pink dots, samples (yellow dots).

Another transect which was used for validation is located between Denmark and Norway in the Skagerrak. It is operated by NIVA.
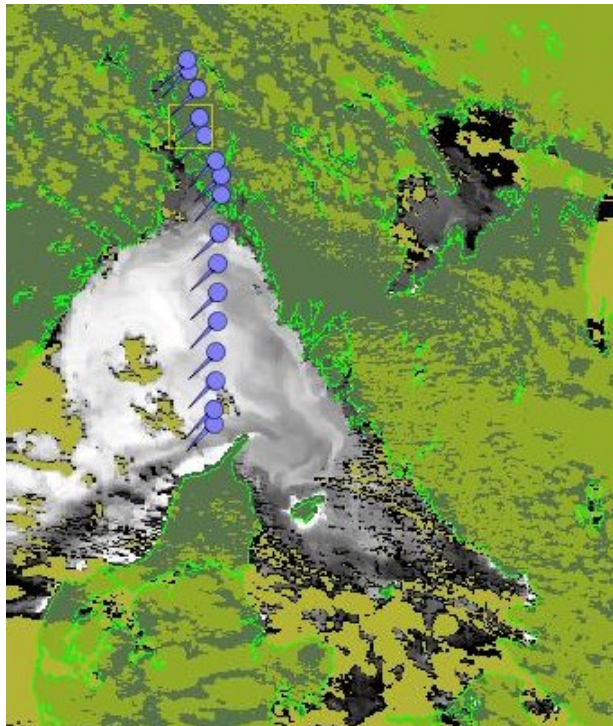
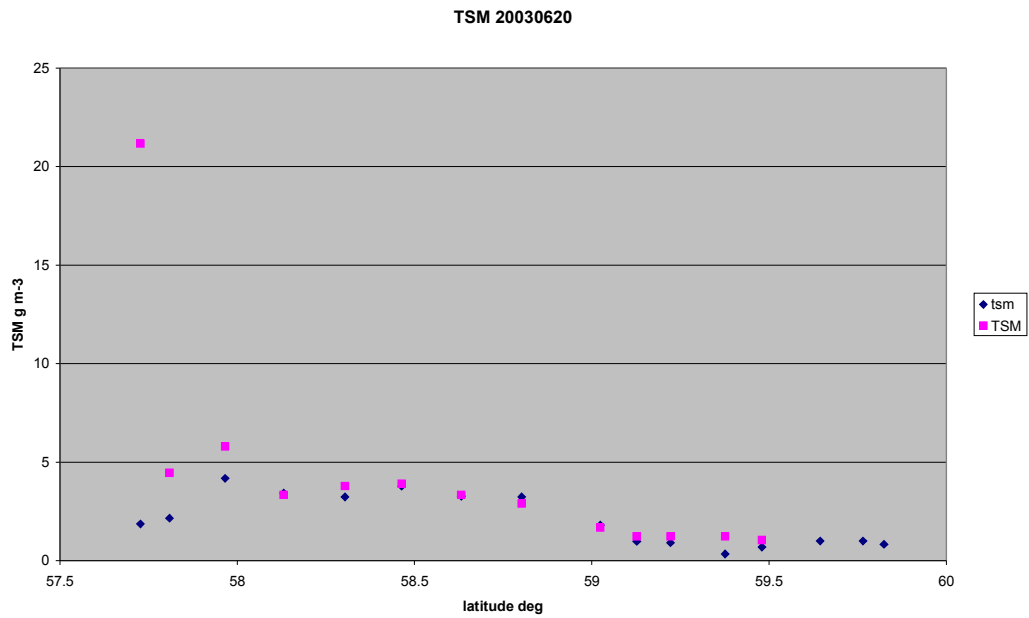Fig. 26: Transect Skagerrak with sampling station (provided by K. Soerensen, NIVA)

Fig. 27: Total suspended matter computed with the C2R algorithm along Skagerrak transect, MERIS (blue) and in situ samples (red dots)
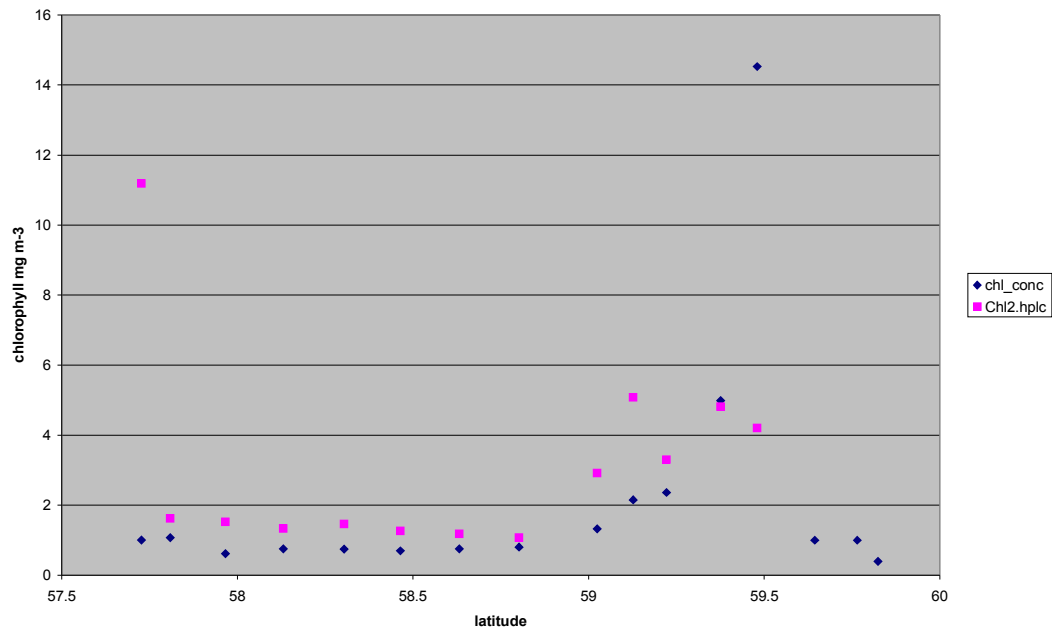
| | SENTINEL-3 L2 PRODUCTS AND ALGORITHM DEFINITION OLCI L2 ATBD Ocean Colour Turbid Water | Document Ref: S3-L2-SD-03-C11-GKSS-ATBD Issue: 2.1 Date: 20100715 Page 41 of 50 |

Fig. 28: Chlorophyll computed with the C2R algorithm along Skagerrak transect, MERIS (blue) and in situ samples (red dots)

8.2   Comparison with algal_1

The standard MERIS data set includes two chlorophyll products. Algal_1 is dedicated to ocean case 1 water; it is computed from three spectral bands of MERIS by using a modified reflectance ratio algorithm. Algal_2 is from the neural network algorithms, which is dedicated to case 2 water. It determines three optical components, absorption coefficient of phytoplankton pigments, absorption coefficient of suspended and dissolved organic components and the scattering by all particles. Algal_2 is then determined as chlorophyll concentration from a_pig using a simple equation, the coefficients of which were derived from samples in various case 2 waters.However, in the ideal case algal_1 and algal_2 should present the same results although both algorithms are different and are based on different data sets.

Here we present a comparison for mainly case 1 water, where the algal_1 algorithm produces valid results. Fig. 29 shows the chlorophyll pattern of algal_1 and algal_2 of the Pacific coast off Oregon (USA) with the same gray level scale, which shows more details than a colour representation.

Fig. 30 is an analyis of 175 scenes (provided by C. Brockmann). It shows the mean chlorophyll concentration of a scene for algal_1 and algal_2.
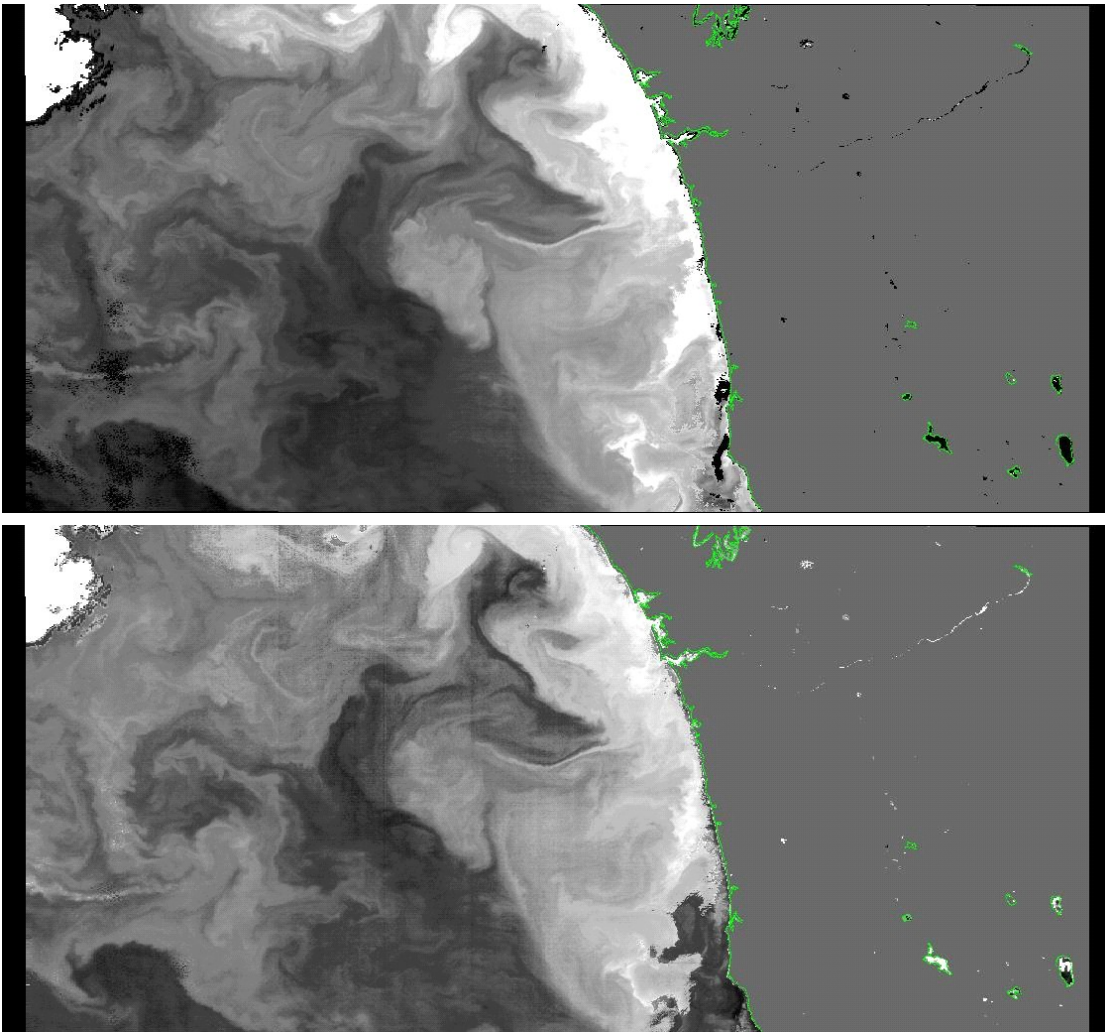
Fig. 29: MERIS 20020921 Pacific ocean off Oregon, upper image algal_1, lower image algal_2

Fig. 30: Mean chlorophyll concentration of 175 scenes algal_1 and algal_2
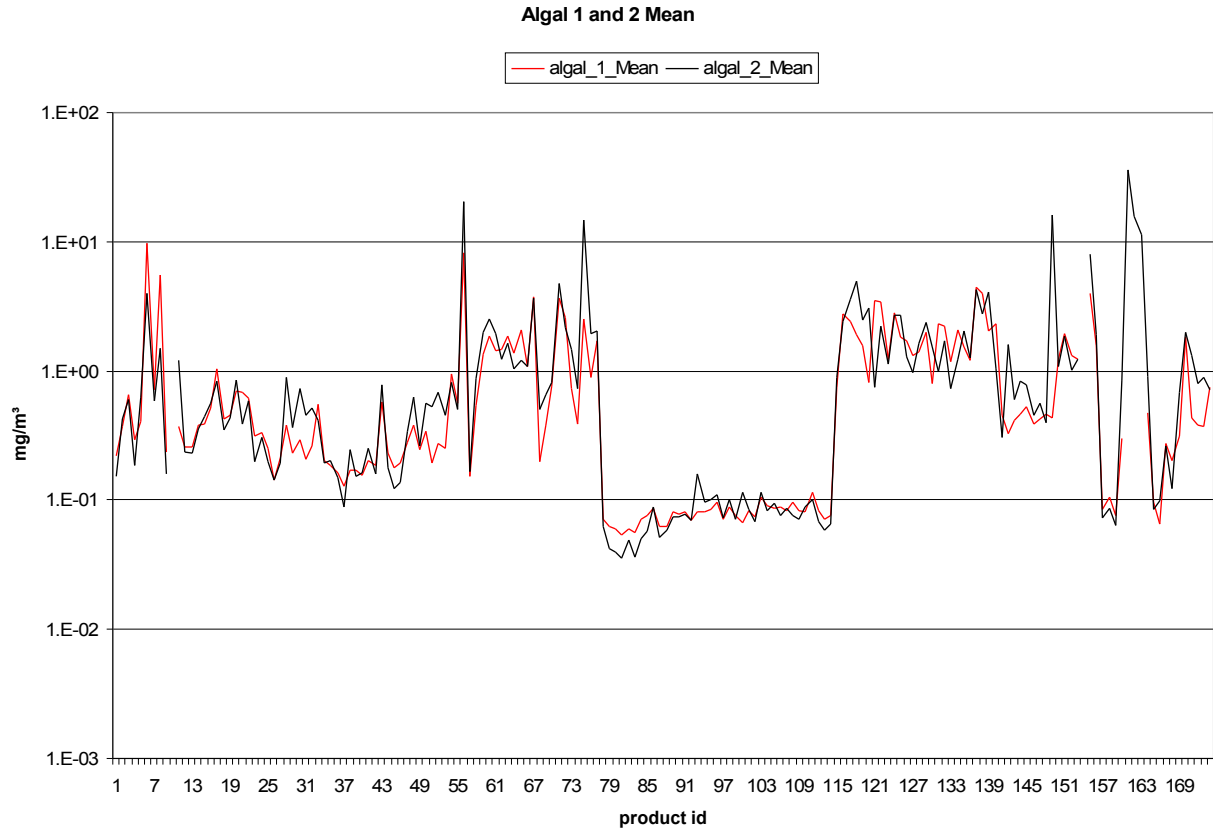
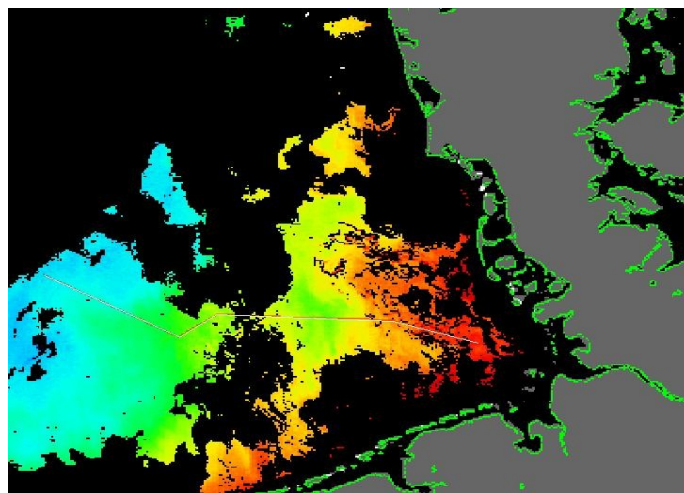Fig. 30: Mean chlorophyll concentration of 175 scenes algal_1 and algal_2

Fig. 31: MERIS scene of the German Bight (North Sea) of 20060704 with transect and masked areas (algal_1 invalid)

Comparison of algal products
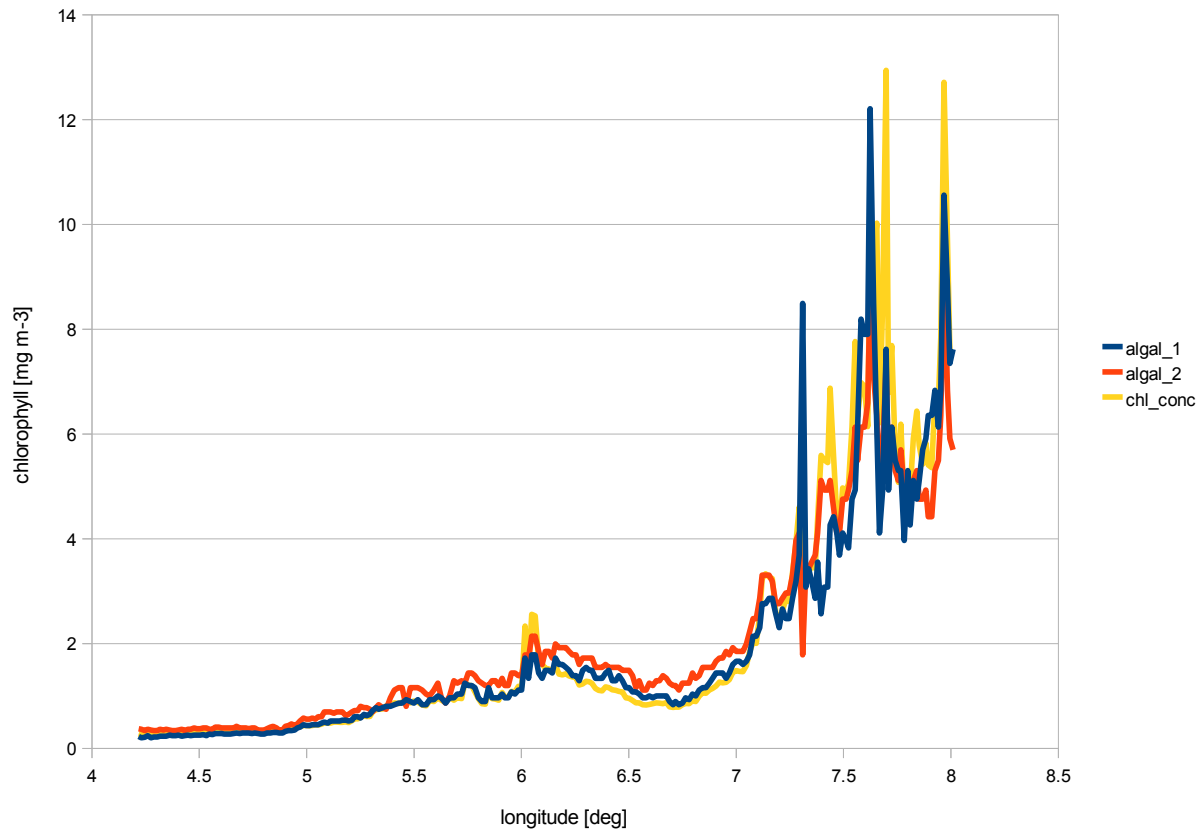
MERIS 20060704 MeGS 22_19

Fig. 32: algal_1, algal_2 and chlorophyll concentration computed with the C2R algorithm along the transec in the German Bight (s. Fig. 31)

Fig. 32 shows the distribution of algal_1, algal_2 and the chlorophyll computed with the C2R algorithm along the transect (s. Fig. 31). algal_1 and algal_2 were processed with MEGS 8.0 with the same standard atmospheric correction procedure, while chl_conc is produced with C2R, which is based on nearly the same neural network as algal_2 but with the neural network atmospheric correction (mentioned in this ATBD also as the alternative case 2 water atmospheric correction).

8.3   Comparison with Secchi Disc measurements

For validation of the z90_max product, which is the depth from which 90% of the reflected (upwelling) irradiance at water surface stems from, a comparison was performed with Secchi Disc measurements in Lake Victoria (East Africa). Fig 33 shows the linear relationship, although both methods measures different quantities.
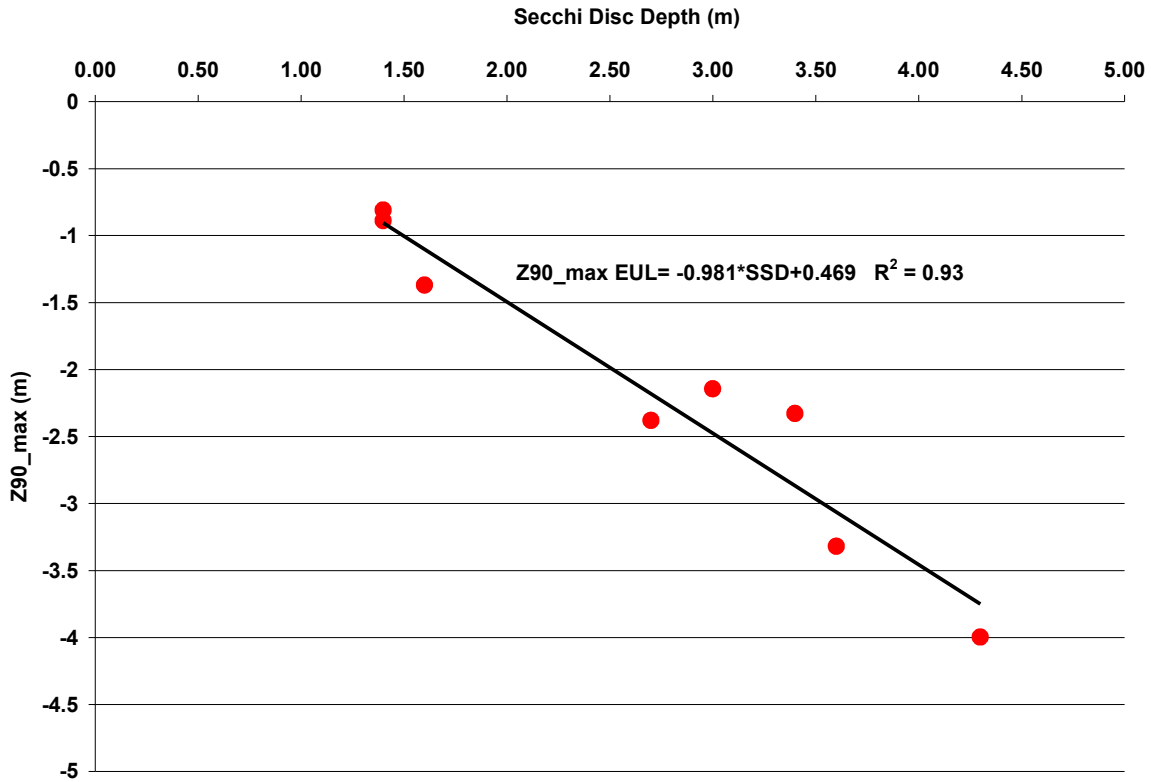
Fig. 33: Relationship between Secchi Disc measurements and z90_max derived from MERIS for Lake Victoria, East Africa

8.4   Comparison with FerryBox data

FerryBoxes are systems to measure water quality variables automatically from ship of opportunities, which run regularly on fixed routes. They provide a good opportunity for validation of satellite data. However, one has to note that only a few data points are match ups. Furthermore, the intake of the water, which is pumped through the measurement system, is located in several meters below surface (normally about 4 m), so that the measurements represent only a layer, which is not the surface. Thus in general one cannot expect a tight agreement between the FerryBox and the satellite data. Also the sensors installed in a FerryBox measure different properties, such as the fluorescence of chlorophyll, which is used as a measure of chlorophyll.

Fig. 34 shows one example of a FerryBox cruise of April 27, 2010. The chlorophyll colour code used for the transects is the same as for the image.
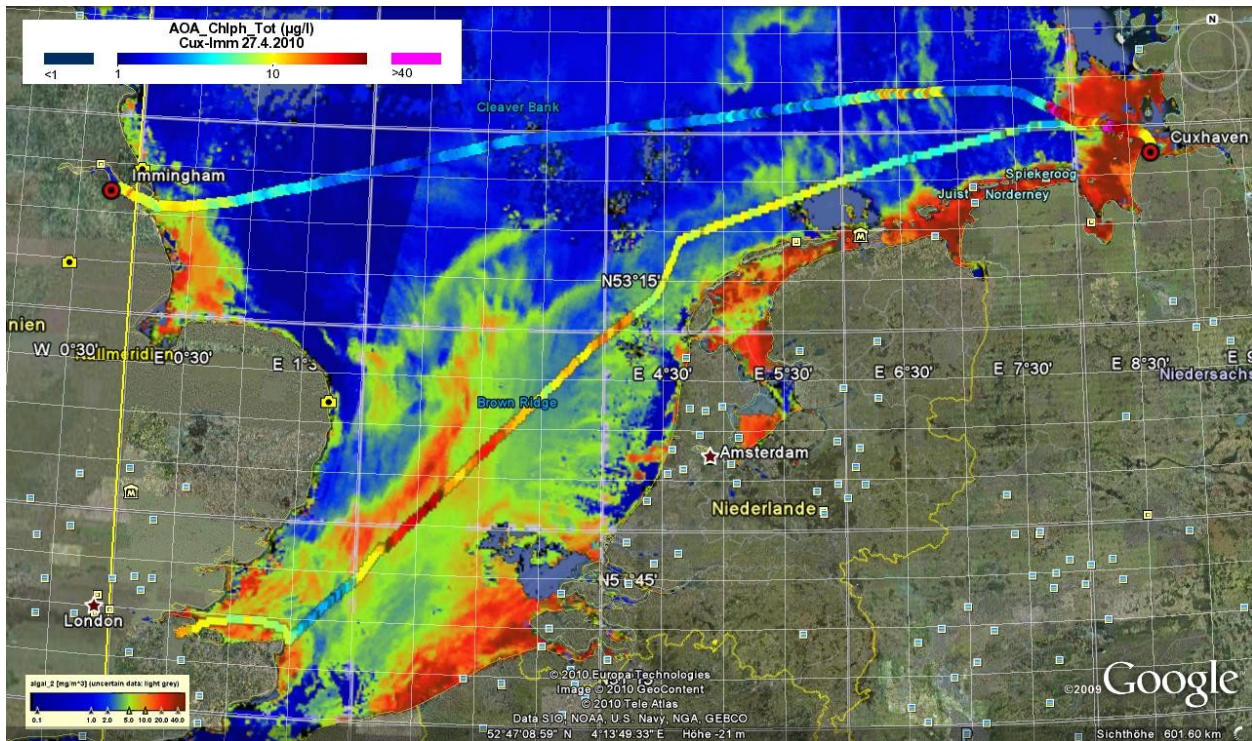
Fig. 34: MERIS scene with transects from the Ferry Box for 20100427, chlorophyll concentrations along the 2 transects have the same colour code

8.5   Validation against test data set of IOCCG Report No. 5

Different case 1 and case 2 water algorithms, which compute IOPs, were analyzed and tested in an IOCCG working group. The results are published in IOCCG Report No. 5. One test was based on simulated data, which were prepared by Z. Lee of the Us Naval Research Laboratory.

It was found that the most robust variables are the total absorption and scattering or backscattering coefficients, because the critical splitting into different components is avoided.

The result for the sun elevation of 30 degrees of the neural network case 2 water algorithm of MERIS is shown here as an example in Fig. 35 and 36.
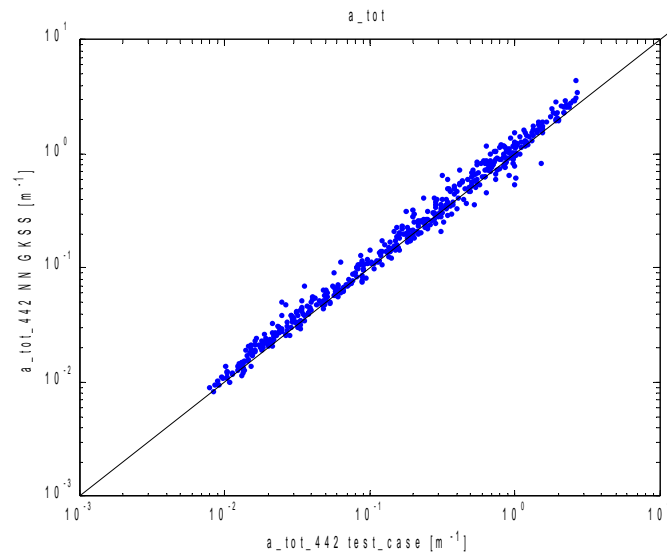
Fig. 35: Scatter plot of total absorption a_tot at 442 nm of IOCCG data set and results of case 2 water algorithm, for a sun zenith angle 30 deg.
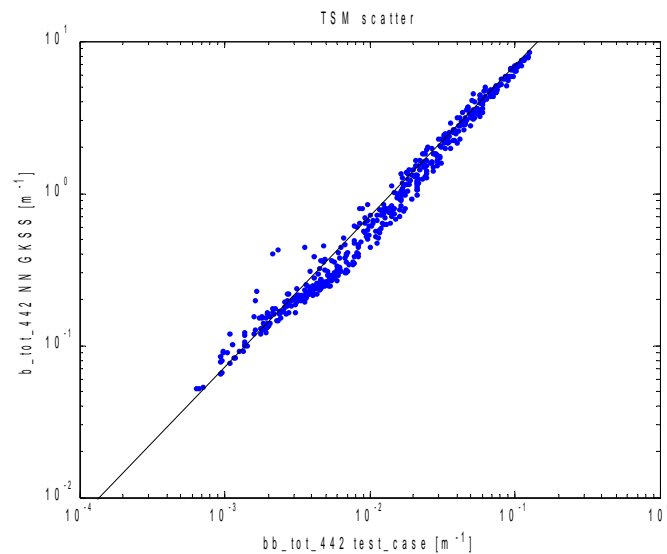
14

Fig. 36: dto. for total scattering

9   REFERENCES

Babin, M., D. Stramski, G. M. Ferrari, H. Claustre, A. Bricaud, G. Obolensky, and N. Hoepffner, 2003, Variations in the light absorption coefficients of phytoplankton, nonalgal particles, and dissolved organic matter in coastal waters around Europe. J. Geophys. Res., vol. 108, NO. C7, 3211

Babin, M., A. Morel, V. Fournier-Sicre, F. Fell and D. Stramski 2003, Light scattering properties of marine particles in coastal and open ocean waters as related to the particle mass concentration. Limnol. Oceanogr., pp. 843–859

Buckton, D., E. O'Mongain and S. Danaher, 1997, The use of Neural Networks for the estimation of oceanic constituents based on the MERIS Instrument. Int. J. Remote Sensing, vol. 20, pp. 1841-1851.

Carder, K. L., F. R. Chen, Z. P. Lee and S. K. Hawes, 1999, Semianalytic Moderate-Resolution Imaging Spectrometer algorithms for chlorophyll a and absorption with bio-optical domains based on nitrate-depletion temperatures. J. Geophys. Res., pp 5303-5421.

Doerffer, R. and J. Fischer, 1994, Concentrations of chlorophyll, suspended matter, and gelbstoff in case II waters derived from satellite coastal zone colour scanner data with inverse modeling methods. J. Geophys. Res., vol. 99, pp. 7457-7466.

Doerffer, R. and H. Schiller, 2000, Neural Network for Retrieval of Concentrations of Water Constituents with the Possibility of Detecting Exceptional out of Scope Spectra. Proc. IGARSS 2000, pp. 714-717.

Hale, G. M., and Querry, M. R. 1973. Optical constants of water in the 200 nm to 200 μm wavelength region. Appl. Opt. 12:555-563.

Hoge, F. E. and P. E. Lyon, 1999, Spectral Parameters of Inherent Optical Property Models: Method for Satellite Retrieval by Matrix Inversion of an Oceanic Radiance Model. Applied Optics, pp. 1657-1662.

Hoogenboom, H.J., A.G. Dekker, J. F. De Haan, 1998, Retrieval of chlorophyll and suspended matter in inland waters from CASI data by matrix inversion. Can. J. Remote Sensing, pp. 144-152

Jain, S. C. and J. R. Miller, 1976, Subsurface water parameters: optimization approach to their determination from remotely sensed water color data. Applied Optics, vol. 15, pp. 886-890.

Krawczyk, H., K. Ebert, A. Neumann, 2004, Algae Bloom Detection in the Baltic Sea with MERIS data. Proc. MERIS User Workshop, Frascati.

Lee, Zhongping, K. L. Carder and R. A. Arnone, 2002, Deriving Inherent Optical Properties from Water Color: a Multiband Quasi-Analytical Algorithm for Optically Deep Waters. Applied Optics, pp, 5755-5772.

Lee, Zhongping (Ed.), IOCCG report NO. 5, in press, www.ioccg.org/reports_ioccg.html

Mobley, C. D., 1994, Light and Water Radiative Transfer in Natural Waters. Academic Press, Inc.

Morel, A., 1974, Optical Properties of pure water and sea water. In Optical aspects of oceanography, ed. By N. G. Jerlov and Nielsen, E. S., pp 1-24, Academic New York.

Morel, A., 1988, Optical modelling of the upper ocean in relation to its biogenous matter content (case 1 waters). J. Geophys. Res., pp 10749-10768.

Morel, A. and D. Antoine, 2000, ATBD 2.9: Pigment Index Retrieval in Case 1 Waters. ESA Doc. No. PO-TN-MEL-GS-0005, pp. 9-1 - 9-26; it can be downloaded from http://isat.esa.int/instruments/meris/pdf/ atbd_2_09.pdf.

Röttgers, R. and R. Doerffer. 2007. Measurements of optical absorption by chromophoric dissolved organic matter using a point-source integrating-cavity absorption meter. Limnol. Oceanogr.: Methods 5: 126–135.

Petzold , T. L., 1972, Volume scattering functions for selected ocean waters. San Diego: Scripps Inst. Oceanogr., Ref 72-78, 79pp.

Pozdnyakov, D., A. Lyaskovsky, H. Grassl and L. Pettersson, 2002, Numerical modelling of transspectral processes in natural waters: implications for remote sensing. Int. J. Remote Sensing, vol. 23, pp. 1581-1607.

Pope, R. and E. Fry, 1997, Absorption spectrum (380-700nm) of pure waters: II. Integrating cavity measurements, Applied Optics, pp 8710-8723.

Schiller, H. and R. Doerffer, 1993, Fast computational scheme for Inverse modeling of multispectral radiances: application for remote sensing of the ocean. Applied Optics, vol. 32, pp. 3280-3285.

Schiller, H. and R. Doerffer, 1999, Neural Network for Emulation of an Inverse Model - Operational Derivation of Case II Water Properties from MERIS data. Int. J. Remote Sensing, vol. 20, pp. 1735-1746.

Schiller, H., 2000, Feedforward-Backpropagation Neural Net Program ffbp1.0. Report GKSS 2000/37, ISSN 0344-9626.

Schiller, H. and R. Doerffer, 2005, Improved Determination of Coastal Water Constituent Concentrations from MERIS Data, IEEE transactions on geoscience and remote sensing, in print.

Siegel, H., M. Gerth, T. Ohde, T. Heene, 2005, Ocean colour remote sensing relevant water constituents and optical properties of the Baltic Sea. Journal of Remote Sensing, pp. 315-330.

Zhang, X., and L. Hu. 2009. Estimating scattering of pure water from density fluctuation of the refractive index. Opt. Expr. 17: 1671-1678.

Zhang, X., L. Hu, and M-X. He. 2009. Scattering by pure seawater: Effect of salinity. Opt. Expr. 17: 5698-5710